scientific reports

Check for updates

OPEN

Incorporation of CuO on the αFe_2O_3 nanoparticles as a heterogeneous catalyst for conversion of waste cooking oil into biodiesel

Atefeh Rezaeifar[1], Mohsen Mansouri[1]✉ & Basir Maleki[2]

This study focused on generating biodiesel from waste cooking oil (WCO) employing an αFe_2O_3/CuO nanocatalyst synthesized via a co-precipitation method. Several characterization techniques, including FTIR, XRD, SEM-EDX, BET, and TEM analyses, were applied to scrutinize the features of the fabricated nanocatalyst. The results confirmed the successful incorporation of CuO into the αFe_2O_3 structure. BET analysis further revealed that the addition of CuO nanoparticles significantly enhanced the catalyst's surface properties, increasing the number of active sites available for transesterification reactions. Besides, the αFe_2O_3/CuO nanocatalyst exhibited a specific surface area of 334 m^2/g, highlighting its high surface availability for catalytic activity. The process was statistically optimized using response surface methodology (RSM) with a Box-Behnken design (BBD) to assess the influence of critical reaction parameters. Vital parameters evaluated included temperature (50–70 °C), methanol/WCO molar ratio (8–14 mol/mol), and catalyst loading (1–3 wt%). Moreover, ANOVA results indicated that the methanol/WCO molar proportion had the most remarkable effect on biodiesel production efficiency, with an F-value of 337.11. Under optimal conditions reaction time of 3 h, methanol/WCO molar ratio of 11, αFe_2O_3/CuO dosage of 2 wt%, and temperature of 60 °C a highest biodiesel yield of 94.27% was achieved. Additionally, the reusability assessment of the αFe_2O_3/CuO nanocatalyst demonstrated notable stability, with only a 12% reduction in efficiency observed over seven cycles. This research demonstrates that αFe_2O_3/CuO nanocatalysts, owing to their unique properties, have the potential to serve as highly effective heterogeneous catalysts for transesterification.

Keywords Co-precipitation, Biodiesel, Transesterification, αFe_2O_3/CuO nanocatalyst, Behnken box design, Reusability

Currently, Fossil fuels including oil, coal, and natural gas, currently account for the majority of global energy consumption[1]. While these energy sources have historically been reliable, they are finite, and the rapid increase in global demand is accelerating their depletion[2]. This escalating demand, coupled with the environmental degradation caused by fossil fuel use, has led to a global energy crisis characterized by dwindling resources, rising fuel costs, and severe environmental challenges[3,4]. To mitigate these issues, there is an urgent need for sustainable, renewable energy sources such as solar, wind, hydrogen, and biofuels, which provide cleaner, more sustainable alternatives. These renewable energy sources not only help conserve resources but also reduce harmful emissions and pollution, thereby addressing critical issues like climate change and global warming[3].

Among renewable alternatives, biodiesel stands out as a particularly promising substitute for conventional diesel fuel. Derived from sustainable sources like vegetable oils, animal fats, and recycled greases, biodiesel is both renewable and biodegradable[3]. Due to its oxygen content (10–12%), biodiesel promotes more complete combustion, resulting in fewer pollutants being emitted compared to fossil diesel[5]. This characteristic reduces the emissions of carbon monoxide, particulate matter, and other harmful pollutants. Moreover, biodiesel does not contain the aromatic compounds found in fossil diesel, which are significant contributors to air pollution, thus positioning biodiesel as a cleaner alternative that aligns with environmental priorities[5,6].

The generation of biodiesel typically involves transesterification, a procedure in which triglycerides from oils are converted into fatty acid alkyl esters[7]. This reaction combines oil with alcohol to produce biodiesel and glycerol, and can occur either with or without the use of a catalyst[8]. In response to growing concerns about

[1]Department of Chemical Engineering, Faculty of Engineering, Ilam University, Ilam, Iran. [2]Department of Chemical Engineering, Esfarayen University of Technology, Esfarayen, North Khorasan, Iran. ✉email: m.mansouri@ilam.ac.ir

food security, there is an increasing interest in utilizing non-edible oils for biodiesel production, such as waste oils, jatropha, karanja, and neem oils. These feedstocks can be cultivated on non-arable land, thus preventing competition with food crops and enhancing the sustainability of biodiesel generation[9,10].

Catalysts play a critical role in improving the yield of biodiesel generation by speeding up chemical reactions and improving yield[11]. Among the various types, heterogeneous catalysts, or solid-phase catalysts, stand out due to several key advantages. These include ease of separation from the reaction mixture, reusability, and a significantly reduced need for post-reaction purification[3,12]. These properties make heterogeneous catalysts especially attractive for large-scale biodiesel production, as they offer a more sustainable and cost-effective solution. A subset of heterogeneous catalysts, nanocatalysts, are particularly effective for biodiesel synthesis[12,13]. Due to their high surface area and unique surface properties, nanocatalysts exhibit superior catalytic efficiency, enabling more complete reactions and higher biodiesel yields. Nanocatalysts like αFe_2O_3 and CuO have gained attention for their enhanced catalytic activity[14]. The αFe_2O_3, with its magnetic properties, facilitates easy separation and recycling, while CuO provides strong catalytic performance in transesterification reactions, improving biodiesel yield and reaction rates[15]. Furthermore, both nanocatalysts can often be reused multiple times without significant loss of activity, which helps in reducing both operational costs and waste generation. This reusability further contributes to making biodiesel production more economically feasible and environmentally sustainable[16]. On the other hand, the αFe_2O_3/CuO catalyst offers distinct advantages over basic catalysts like CaO and MgO, as well as acidic or bifunctional catalysts[15]. Unlike CaO and MgO, αFe_2O_3/CuO exhibits superior thermal stability and enhanced catalytic activity due to the synergistic interaction between Fe and Cu ions, which improves electron transfer kinetics. Its dual redox-active sites also contribute to higher biodiesel yields, particularly with challenging feedstocks[16]. However, its catalytic performance under acidic or water-rich conditions may be limited compared to acidic or bifunctional catalysts, as αFe_2O_3/CuO shows lower tolerance to free fatty acids (FFAs) and water. In contrast, while CaO and MgO are cost-effective and simple to use, their sensitivity to FFAs often results in soap formation, significantly reducing efficiency[16,17]. Literature highlights αFe_2O_3/CuO's potential as a robust, versatile catalyst for biodiesel synthesis. Maleki et al.[15]. optimized biodiesel production using αFe_2O_3/ZnO nanocatalyst, achieving 83.19% yield with improved pour point. Catalyst showed reusability across seven cycles under optimal conditions. Talebi et al.[16] studied Mg-Zr doping on CaO catalysts for biodiesel production, achieving 96.07% FAME with 7.5 wt% Mg-Zr/CaO under optimal conditions. Olubunmi et al.[17]. optimized biodiesel generation from beef tallow employing calcium oxide catalyst, identifying significant factors. The optimal conditions achieved 61% FFA, with the quadratic model showing high predictive accuracy ($R^2 = 0.9592$).

The Box-Behnken based on response surface methodology (BBD-RSM) plays a crucial role in optimizing biodiesel production processes by enabling efficient and precise modeling of complex, multivariable systems[15,18]. This statistical approach minimizes the number of required experimental trials, saving both time and resources while allowing researchers to examine interactions among key variables, such as temperature, catalyst loading, reaction time, and feedstock composition[19,20]. In biodiesel production, Box-Behnken RSM is particularly valuable for identifying optimal conditions that maximize yield, purity, and quality. Additionally, it provides insights into how each parameter influences overall process efficiency[21]. By establishing these optimal conditions, the Box-Behnken design supports cost-effective and scalable biodiesel production, aiding in the shift toward cleaner energy alternatives and reducing dependence on fossil fuels[22]. On the other hand, BBD-RSM has several limitations. It requires careful selection of input ranges to avoid misleading outcomes, and it becomes inefficient when optimizing systems with more than three factors, as the number of required runs increases significantly[20,21]. Additionally, it may struggle to model highly nonlinear relationships accurately and assumes uniform variability across all levels, which may not always hold true[22]. These limitations can affect its effectiveness, particularly in complex biodiesel synthesis processes.

The present study aims to synthesize biodiesel from WCO using the highly reactive αFe_2O_3/CuO nanocatalyst. To thoroughly characterize the αFe_2O_3/CuO nanocatalyst, various analytical techniques were employed, including Brunauer-Emmett-Teller (BET) surface area analysis, X-ray diffraction (XRD), Fourier-transform infrared spectroscopy (FTIR), energy-dispersive X-ray (EDX) spectroscopy, transmission electron microscopy (TEM), and scanning electron microscopy (SEM). These methods were used to assess the structural and surface properties of the nanocatalyst. Additionally, the Box-Behnken design (BBD) combined with response surface methodology (RSM) was applied to study and optimize the effect of key process variables, such as temperature, catalyst loading, and reaction time, on biodiesel yield. The recyclability and stability of the αFe_2O_3/CuO nanocatalyst were also evaluated over multiple cycles, providing insights into its industrial application potential for sustainable biodiesel production.

Materials and methods

Chemicals

The materials employed in this research included $Fe(NO_3)_3{\cdot}9\ H_2O$ (Merck, ≥98%), $Cu(NO_3)_2{\cdot}2\ H_2O$ (Merck, ≥98), methanol, NaOH (Merck, ≥99), and waste cooking oil (WCO). $Fe(NO_3)_3{\cdot}9\ H_2O$ and $Cu(NO_3)_2{\cdot}2\ H_2O$ served as precursors for synthesizing the αFe_2O_3 and CuO nanocatalysts, respectively. Methanol (Merck, ≥99.8%) was used as the alcohol component in the transesterification process, while NaOH acted as the stimulus to precipitate of particles. WCO was chosen as an economical and sustainable feedstock for biodiesel production. The physical and chemical features of the oil used are provided in Table 1. This table outlines important characteristics, including viscosity, density, acid value, free fatty acid (FFA) content, and iodine value of the WCO. These properties are essential in assessing the oil's suitability for biodiesel production, as they directly affect the efficiency of the transesterification process and the quality of the produced biodiesel. Comprehending these parameters helps optimize the biodiesel synthesis process and ensures the desired fuel features.

Feature	Unit	Reported value
Density (at 15 °C)	(gr/cm^3)	0.924
Average molecular weight	(g/mol)	863.5
Kinematic viscosity (at 40 °C)	(cp.)	39.43
Flash point	(°C)	230
Calorific value	MJ/kg	39.12
Moisture	(%)	>0.1
Saponification value	mg KOH/g	196.84
Acid value	mg KOH/g	5.72
Free fatty acid (FFA)	(%)	1.59

Table 1. Report of the results of the features of the WCO.

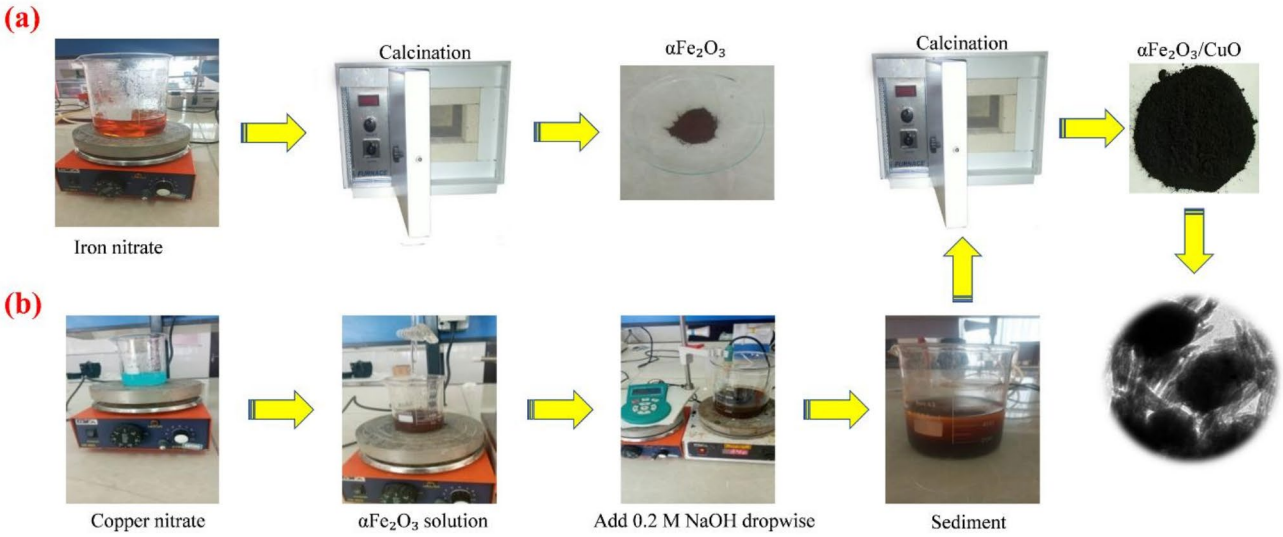

Fig. 1. Schematic of the synthesis steps of (**a**) αFe_2O_3 and (**b**) αFe_2O_3/CuO.

Synthesis of αFe2O3

αFe_2O_3 nanoparticles were synthesized using the co-precipitation method, a straightforward approach to producing uniform nanoparticles. Initially, the temperature of a magnetic stirrer was set to 50 °C, providing optimal conditions for the reaction. A total of 50 g of iron nitrate ($Fe(NO_3)_3{\cdot}9\ H_2O$) was accurately weighed and dissolved in 1 L of distilled water in a beaker, followed by continuous stirring for 30 min to ensure complete dissolution. Subsequently, a 0.2 M sodium hydroxide (NaOH) solution was added dropwise to the solution to gradually increase the pH to 9, facilitating the formation of iron hydroxide precipitates. This mixture was then allowed to settle, and the precipitate was thoroughly washed multiple times with distilled water to eliminate any residual impurities. The cleaned precipitate was dried in an oven at 100 °C for 24 h to remove moisture. Finally, the dried dark brown precipitate underwent calcination at 500 °C for 3 h, converting it into crystalline αFe_2O_3 nanoparticles with improved purity and stability.

Synthesis of αFe2O3/CuO nanocatalyst

To synthesize the αFe_2O_3/CuO nanocatalyst with a 1:1 molar ratio via the co-precipitation method, copper nitrate dihydrate ($Cu(NO_3)_2{\cdot}2\ H_2O$) was initially dissolved in distilled water within a 500 mL beaker at 50 °C, under constant stirring with a magnetic stirrer. After the copper nitrate fully dissolved, a measured amount of pre-synthesized αFe_2O_3 was added to the solution, followed by continuous stirring for 1 h to ensure uniform dispersion. A 0.2 M sodium hydroxide solution was then added dropwise until the pH reached approximately 10, facilitating the co-precipitation of metal hydroxides. Following an additional 0.5 h of stirring, the mixture was allowed to settle, and the precipitate was thoroughly washed multiple times with an ethanol-distilled water mixture to eliminate residual impurities. The cleaned precipitate was then dried in an oven at 100 °C for 24 h. Finally, the dried material was calcined at 500 °C for 3 h in a furnace (Shimaz Co, Iran) to obtain the αFe_2O_3/CuO nanocatalyst. The synthesis steps for each catalyst are depicted in Fig. 1.

Characterization of AFe_2O_3/CuO nanocatalyst

To determine the phase composition and crystallinity of the synthesized catalysts, XRD analysis was conducted using a Rigaku 1160 device. Additionally, SEM (FlexSEM 1000 II VP-SEM) was performed to observe the

morphology and particle size of the catalyst. TEM analysis (JEOL-JEM-F200 model) was utilized to evaluate the shape and size of the nanocatalyst particles. FTIR analysis (ALPHA II Compact FT-IR Spectrometer) was applied to identify functional groups and chemical bonding in the catalysts. Furthermore, BET analysis (BELSORP MR1 model) was carried out to determine the surface area, pore volume, and pore size distribution of the catalyst. Finally, TGA analysis (HZ2329 TGA thermal analyzer) was employed to assess the thermal stability of the catalyst.

Transesterification of WCO by AFe_2O_3/CuO nanocatalyst

In this reaction, triglycerides in WCO were converted into methyl esters and glycerol using methanol and an αFe_2O_3/CuO nanocatalyst. The reaction conditions included a constant reaction time of 3 h, a temperature range of 50–70 °C, a methanol/ WCO molar ratio of 8–14 mol/mol, and a catalyst dosage of 1–3 wt%. Initially, the appropriate amounts of catalyst and methanol were introduced into the reactor, and to initiate the transesterification, 30 g of preheated WCO was added to the catalyst-methanol mixture. The mixture was stirred at 700 rpm to ensure thorough interaction of the reactants. Upon completing the reaction, heating and stirring were stopped, and the reactor with its condenser was removed from the heating bath. The reaction mixture was then centrifuged at 4000 rpm for 15 min to efficiently separate the solid catalyst from the biodiesel and glycerol mixture. The liquid phase was transferred to a 250 mL decanter funnel and catnapped for one day for complete phase segregation. After settling, the biodiesel-rich layer was collected from the top, with glycerol settling at the bottom. The biodiesel phase was then dried in an oven at 80 °C for 1 h to evaporate residual methanol, resulting in a purified biodiesel product. Biodiesel yield (BY) was then achieved via the below Eq. (1)[15,21]:

$$BY\ (\%) = \frac{gr\ of\ biodiesel\ generated}{gr\ of\ WCO} \times\ 100 \tag{1}$$

While Eq. (1) was employed to calculate the biodiesel yield, the methyl ester content was determined utilizing gas chromatography (GC) analysis (Agilent, 6890 N-5973, USA) in accordance with ASTM D6584 standards. The GC method enables accurate quantification of methyl esters and ensures compliance with biodiesel quality standards.

Experimental design via BBD-RSM

Statistical methods are crucial for improving the efficiency and sustainability of biodiesel production processes, providing a structured, data-driven approach to optimizing key variables. In this study, the Box-Behnken design (BBD), a powerful statistical tool within Response Surface Methodology (RSM), was applied to assess and optimize the effects of three key factors on biodiesel yield from WCO[19,21]. The selected factors included the methanol/ WCO molar ratio (8–14 mol/mol), reaction temperature (50–70 °C), and catalyst loading (1–3 wt%). These variables were selected based on methanol boiling point, transesterification efficiency, economic feasibility, preliminary experiments, and prior studies for optimizing biodiesel generation. Using Design Expert Software, the study efficiently evaluated these variables to optimize biodiesel production with an αFe_2O_3/CuO nanocatalyst. The primary aim was to identify the optimal conditions for maximizing biodiesel yield. The BBD-based RSM approach allowed for a detailed examination of both individual factor effects and their interactions, providing deeper insights into how these variables work together to influence the process. Additionally, the experimental conditions and their respective ranges were outlined in Table 2, following the BBD design framework. This organized approach ensured that all critical factors were systematically considered during the optimization process, leading to more effective and reliable biodiesel production outcomes.

Results and discussion

Characterization of AFe_2O_3/CuO

Figure 2 displays the FTIR spectra of the αFe_2O_3/CuO nanocomposite within the wavenumber range of 4000–400 cm^{-1}, showcasing vibrational characteristics that reflect the material's functional groups. The sharp and intense peaks observed in the spectrum signal distinct structural features, with notable changes in stretching vibrations. Prominent absorption bands at approximately 3500 cm^{-1} and 1600 cm^{-1}, specifically at 3442 cm^{-1} and 1629 cm^{-1}, are indicative of the stretching and bending vibrations of adsorbed water molecules, signifying strong water interaction with the nanocomposite[23,24]. The spectrum also reveals metal-oxygen vibrational modes O-M-O, M-O, and M-O-M (where M represents Fe or Cu) in the 800–500 cm^{-1} range, which provide crucial information about the bonding frameworks within the nanocomposite. In the higher wavenumber range of 3700–3200 cm^{-1}, O-H stretching vibrations are evident, corresponding to hydroxide layers and intertwined water molecules. This feature underscores the hydrophilic nature and water-associated interactions of the composite material[24,25]. Additionally, a sharp peak at 1383 cm^{-1} is ascribed to the stretching and bending vibrations of nitrate anions, pointing to residual or incorporated nitrate species from the synthesis process. This

Variables	Symbol	Units	Low (−1)	Middle (0)	High (+1)
Catalyst dosage	X_1	wt%	1	2	3
Methanol/oil ratio	X_2	molar	8	11	14
Temperature	X_3	°C	50	60	70

Table 2. Transesterification factors and their range in biodiesel synthesis.

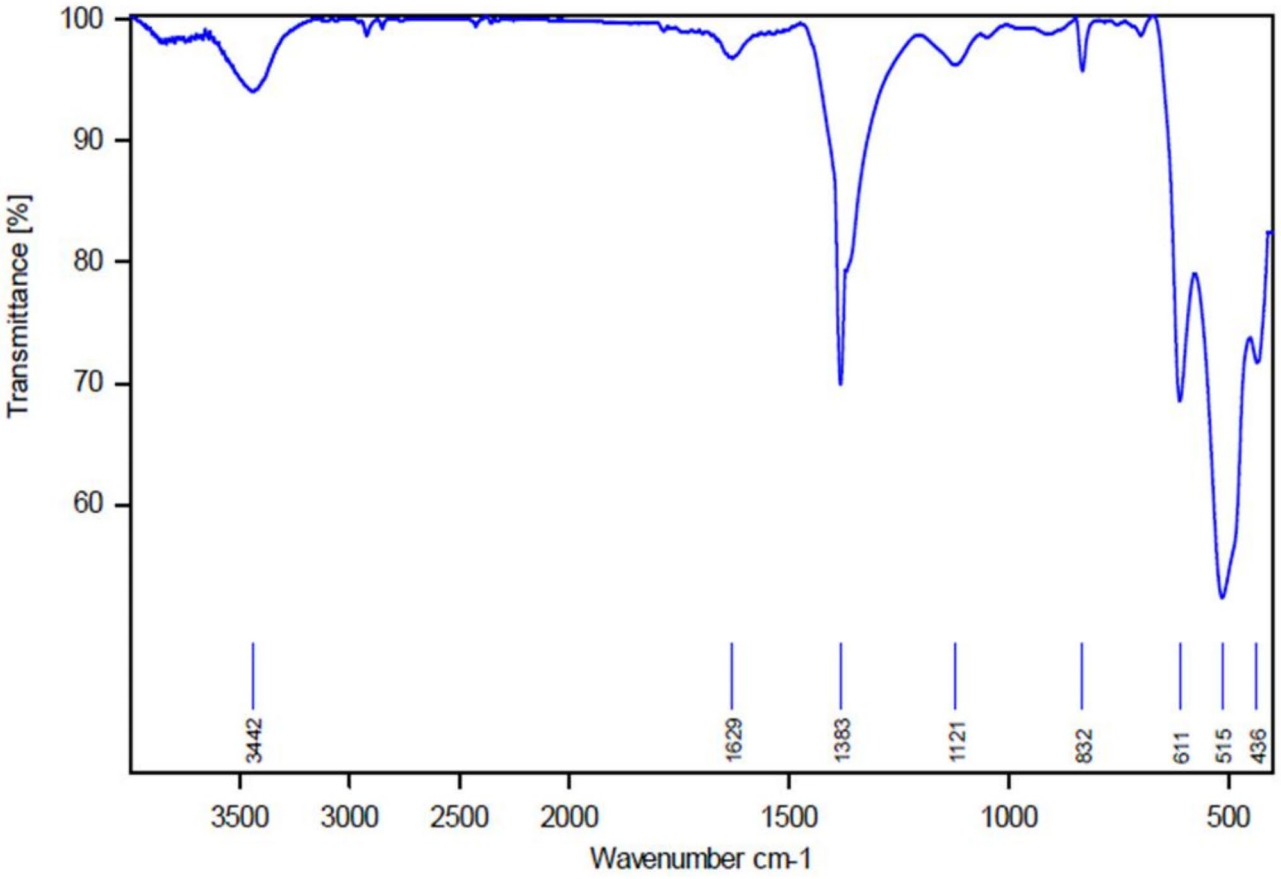

Fig. 2. FTIR analysis curve for the αFe_2O_3/CuO nanocomposite.

detailed spectral analysis highlights the complex vibrational dynamics and structural intricacies of the αFe_2O_3/CuO nanocomposite, offering insights into its chemical interactions and potential functional properties[26,27].

The XRD pattern of the synthesized αFe_2O_3/CuO nanocomposite, shown in Fig. 3, reveals the presence of two distinct crystalline phases, hematite (αFe_2O_3) and tenorite (CuO). The hematite phase, featuring a hexagonal crystal structure, is the predominant crystalline phase in the composite, while the tenorite phase, characterized by a monoclinic structure, is also consistently observed[25]. Key diffraction peaks corresponding to the hematite phase are prominently detected at 2θ values of 19.64°, 33.37°, 35.83°, 54.24°, and 62.62°, aligning with its characteristic reflections and confirming its crystalline integrity. Similarly, the tenorite phase exhibits peaks at 2θ values of 38.9°, 48.7°, 66°, and 68.08°, which are consistent with its standard diffraction patterns[27,28]. The XRD analysis confirms the successful synthesis of the αFe_2O_3/CuO nanocomposite, with distinct and well-defined crystalline phases for both components. These results highlight the effective integration of hematite and tenorite, ensuring structural compatibility and enhancing the composite's potential for catalytic and functional applications[29,30].

The SEM image of the αFe_2O_3/CuO nanocomposite, presented in Fig. 4, reveals a morphology characterized by small spherical particles of varying sizes attached to larger cubic crystals. The αFe_2O_3 acts as a structural support, providing a surface for the CuO particles to adhere to, contributing to the nanocomposite's overall morphology. Most nanoparticles are observed to be smaller than 100 nm, highlighting their nanoscale dimensions. However, agglomeration of the nanoparticles is noticeable in the image. This agglomeration arises from the high surface energy of the nanoparticles, which increases with their large surface-to-volume ratio. To reduce surface energy, these nanoparticles tend to cluster together, forming agglomerates[29]. Although agglomeration may limit the accessible active surface area for catalytic reactions, the robust interaction between αFe_2O_3 and CuO likely compensates for this by promoting effective dispersion at the microscopic level. This structural synergy is expected to improve the catalytic activity of the nanocomposite, despite the observed particle clustering.

EDX analysis was conducted to qualitatively and quantitatively determine the elemental composition of the αFe_2O_3/CuO nanocomposite, with the results presented in Fig. 5 (a) and Table 3. The analysis confirmed the presence of the elements oxygen (O), iron (Fe), and copper (Cu) within the nanocomposite. As shown in the data, copper emerged as the dominant element, exhibiting a weight% exceeding 62% and an atomic percentage of approximately 36%. Oxygen and iron were also present in significant amounts, contributing to the overall composition of the nanocomposite. The high Cu content underscores its substantial role in the material's structural and functional properties. Moreover, the absence of any extraneous peaks or unexpected elements in the EDX spectrum validates the purity of the synthesized nanocomposite, confirming that no impurities

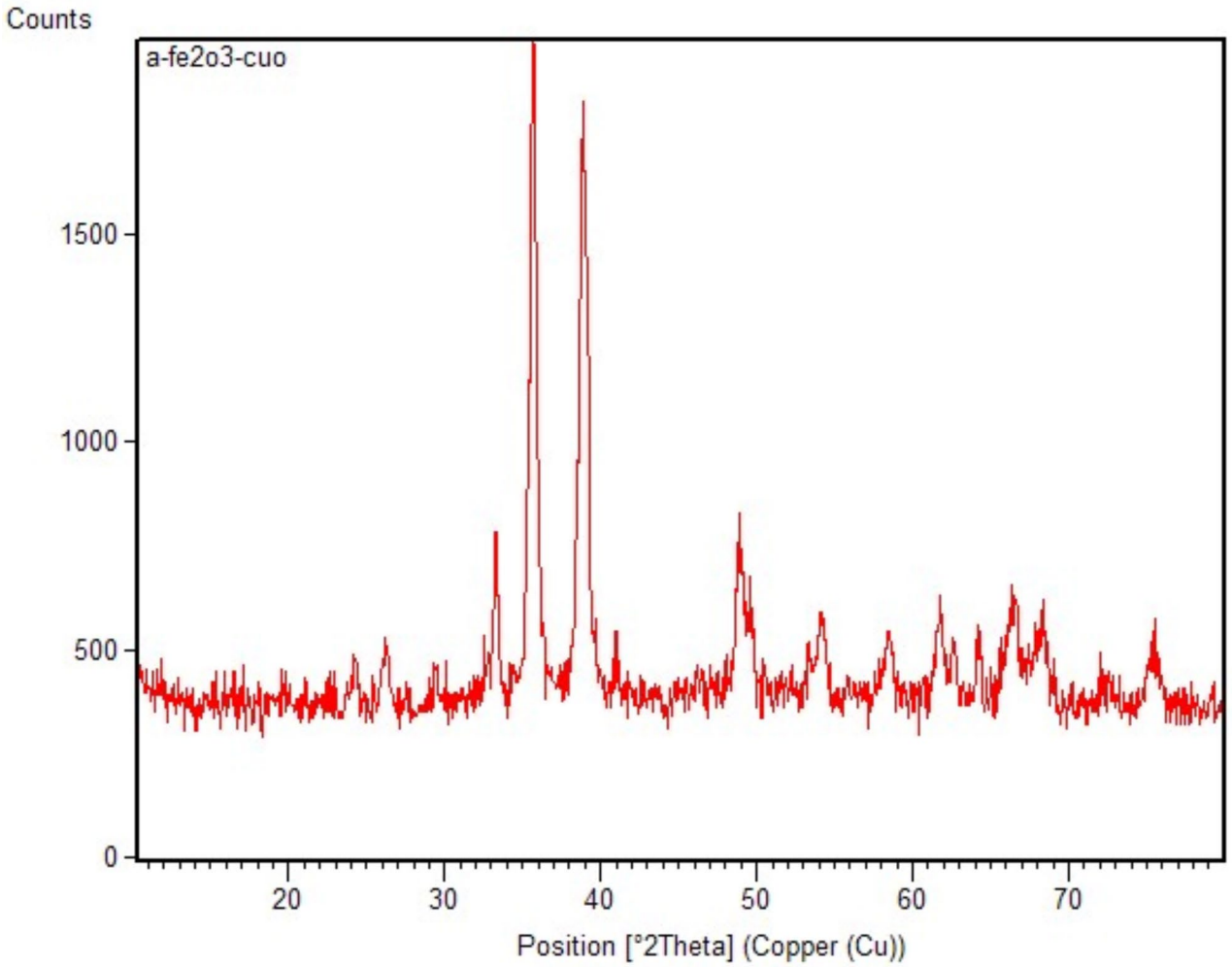

Fig. 3. XRD pattern of αFe_2O_3/CuO nanocomposite.

were introduced during the synthesis process. This ensures the reliability of the αFe_2O_3/CuO nanocomposite for potential applications, particularly in catalytic systems, where purity and precise elemental composition are critical for performance[30,31].

The TGA results for αFe_2O_3 and αFe_2O_3/CuO nanocatalysts are presented in Fig. 5 (b), demonstrating their weight loss profiles as a function of temperature. The data reveal that Fe_2O_3 nanoparticles experience a total weight loss of 23.7 wt% when heated to approximately 800 °C, whereas αFe_2O_3/CuO nanoparticles exhibit a higher weight loss of 33.9 wt% under the same conditions. This indicates that αFe_2O_3/CuO nanoparticles have lower thermal resistance compared to pure αFe_2O_3 nanoparticles. The observed weight loss can be linked to distinct thermal events occurring over specific temperature ranges. The initial weight loss between 50 °C and 200 °C corresponds to the removal of physically adsorbed water molecules and surface hydroxyl groups[28,30]. The next phase, spanning 200 °C to 400 °C, is likely associated with the decomposition of organic compounds within the catalyst matrix. Finally, the significant weight loss observed between 400 °C and 800 °C can be attributed to the thermal breakdown of more stable organic components, their conversion into gaseous products, and the possible degradation or collapse of the catalyst structure[30,31]. The differences in thermal behavior between αFe_2O_3 and αFe_2O_3/CuO nanocatalysts may be attributed to the incorporation of CuO, which could influence the material's structural integrity and alter its thermal decomposition pathways.

The BET analysis of the synthesized αFe_2O_3/CuO nanocatalyst, depicted in Fig. 6, demonstrates its superior surface properties, essential for catalytic processes like transesterification[32]. The integration of CuO nanoparticles enhances the specific surface area and increases the density of active sites. The nanocatalyst exhibits a BET surface area of 74.45 $m^2\ g^{-1}$, reflecting its highly porous structure and substantial adsorption capacity. Using the BJH method, the pore size distribution analysis reveals a pore size of about 1.2 nm and an average pore diameter of 3.2 nm, classifying the material as mesoporous. This mesoporosity is advantageous for catalytic reactions, as the moderate pore size promotes efficient molecular diffusion and accessibility to active sites[33,34]. At a relative pressure of $P/P_0 = 0.990$, the total pore volume is 0.037666 cm^3 (STP) g^{-1}, highlighting its high adsorption potential. The nanocatalyst demonstrates robust nitrogen gas adsorption at high relative pressures, with a maximum adsorbed gas volume of 429.24 cm^3 (STP) g^{-1} at a relative pressure of 0.9906. Conversely,

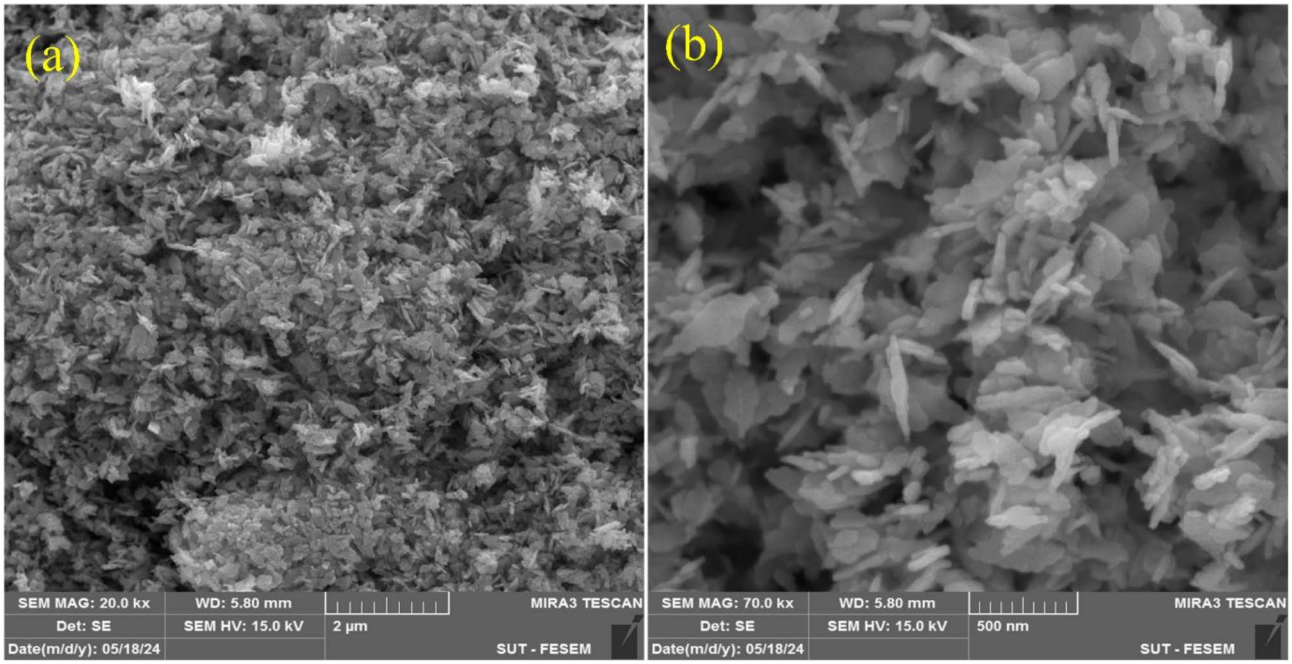

Fig. 4. FESEM images for αFe_2O_3/CuO nanocomposite (**a**) 2 µm and (**b**) 500 nm.

the adsorbed gas volume diminishes at lower relative pressures, reaching 129.13 cm^3 (STP) g^{-1} at a relative pressure of 0.2969. These findings confirm that the αFe_2O_3/CuO nanocatalyst exhibits exceptional surface and pore characteristics, ideal for catalytic applications[34]. Its high surface area, optimal mesoporous structure, and significant adsorption-desorption capacity enhance the interaction between the catalyst and reactants, enabling efficient catalytic performance for biodiesel generation[33,35].

The TEM analysis of the αFe_2O_3/CuO nanocatalyst provided detailed insights into its structural properties at the nanosize (Fig. 7). The images revealed well-dispersed αFe_2O_3 particles adorned with CuO nanoparticles, confirming the successful synthesis of the composite material. The αFe_2O_3 nanoparticles exhibited a needle-like morphology, while the CuO nanoparticles appeared as spherical structures attached to the surfaces of the αFe_2O_3 particles. The particle sizes were predominantly below 50 nm, aligning with the observations from SEM analysis. Nevertheless, a certain degree of particle agglomeration was observed, likely attributable to the high surface energy of the catalyst. The TEM analysis also displayed distinct lattice fringes, signifying the crystalline nature of both αFe_2O_3 and CuO. This structural synergy between αFe_2O_3 and CuO is expected to significantly enhance the catalytic efficiency of the nanocatalyst in biodiesel production.

Statistical analysis for biodiesel synthesis via BBD-RSM

The experimental data for biodiesel production were analyzed using RSM) based on BBD approach, employing Design Expert 10 software. The results, summarized in Table 4, highlight the biodiesel production efficiency achieved under various process conditions. The findings indicate that key variables, like the methanol/WCO molar proportion, reaction temperature, and catalyst dosage, significantly impact production efficiency[15,36]. The analysis emphasizes the importance of optimizing these parameters to maximize biodiesel yield. Through the RSM-BBD methodology, the study effectively explored the interactions among these factors, providing a detailed understanding of their combined effects on the transesterification process. This systematic approach enables the identification of optimal operating conditions, contributing to improved efficiency and scalability of biodiesel production processes[37,38].

Furthermore, Eq. (2) demonstrates exceptional accuracy, as evidenced by the low coefficient of variation (C.V.) value of 0.97, signifying minimal deviation between the predicted and experimental data points[38]. This low C.V. value highlights the robustness and reliability of the model in accurately capturing the interactions among process variables and predicting biodiesel production efficiency with high precision[37,39]. Such accuracy underscores the effectiveness of the applied statistical methodology in optimizing the transesterification process, ensuring consistent and efficient biodiesel production products.

$$\begin{aligned}\text{Biodiesel Yield } (\%) = {} & +93.98 + 2.12\ X_1 + 1.28\ X_2 + 1.56\ X_3 - 2.64\ X_1X_2 + 3.90\ X_1X_3 \\ & - 0.21\ X_2X_3 - 110.05\ X_1^2 - 6.48\ X_2^2 - 80.03\ X_3^2\end{aligned} \tag{2}$$

The ANOVA results, as presented in Table 5, highlight the significant interaction between the methanol/WCO molar ratio (X_1) and temperature (X_3) in influencing the FAME yield. This finding highlights the critical role of the methanol/WCO molar ratio in optimizing biodiesel production efficiency. The interaction between these two parameters suggests that adjusting the methanol/WCO molar ratio in conjunction with temperature can

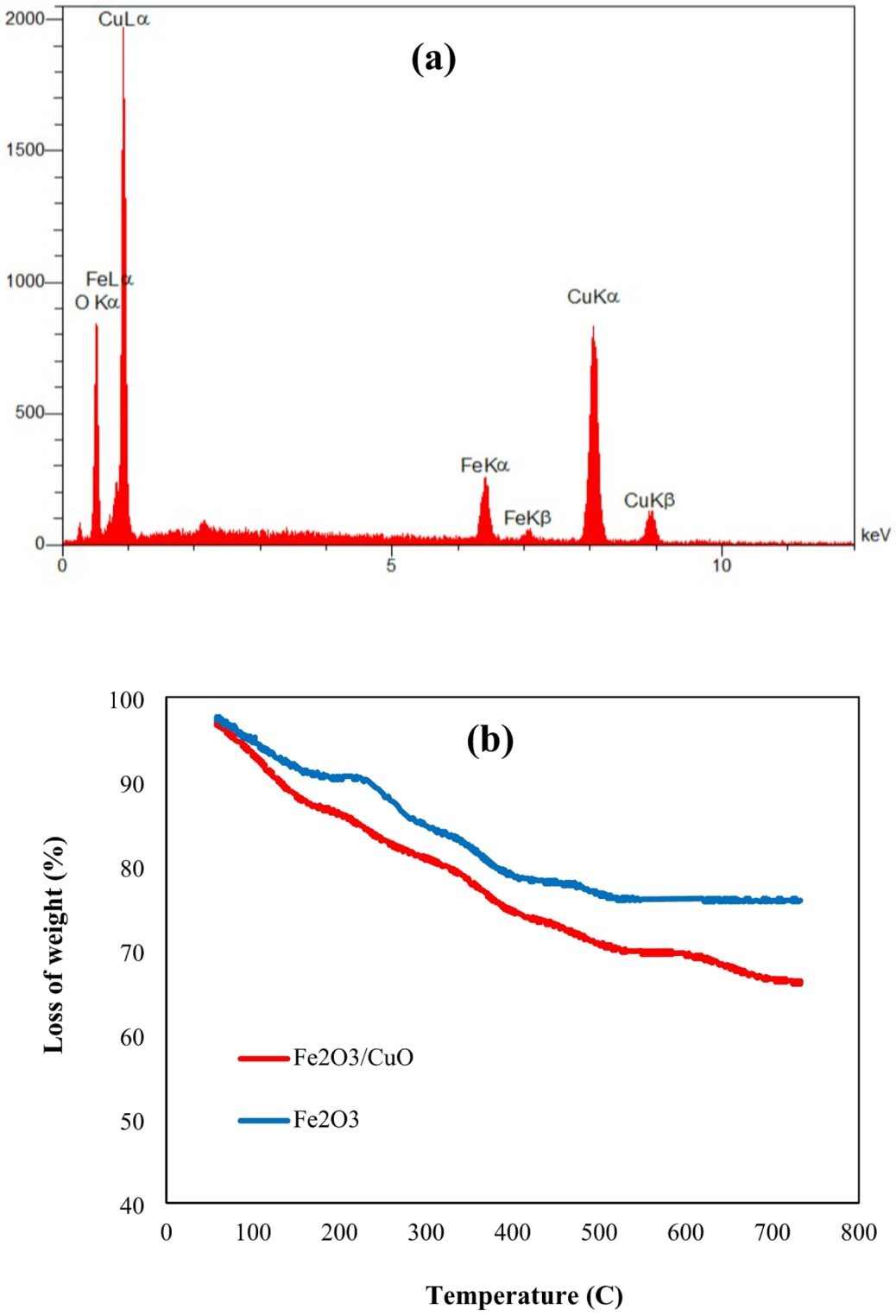

Fig. 5. EDX results (**a**) and TGA results (**b**) for synthesized nanocatalysts.

significantly improve the transesterification process, thereby maximizing biodiesel yield. Moreover, Table 5 further provides insight into the relative importance of the reaction parameters. The methanol to WCO ratio (F-value = 337.11), reaction temperature (F-value = 182.67) and catalyst amount (F-value = 123.90) emerged as the most influential variables, emphasizing their substantial impact on biodiesel yield[40]. All three parameters demonstrated high F-values, indicating that variations in these factors result in considerable changes in the response variable (FAME yield). The low p-values (< 0.0001) for all variables confirm the statistical significance of these factors, reinforcing their critical role in determining the efficiency of the biodiesel generation process[41].

Element	Xray	Weight%	Atomic %
O	Ka	23.08	53.75
Fe	Ka	14.35	9.58
Cu	La	62.56	36.68
Total		100.00	100.00

Table 3. Elemental analysis of αFe_2O_3/CuO obtained from EDX analysis.

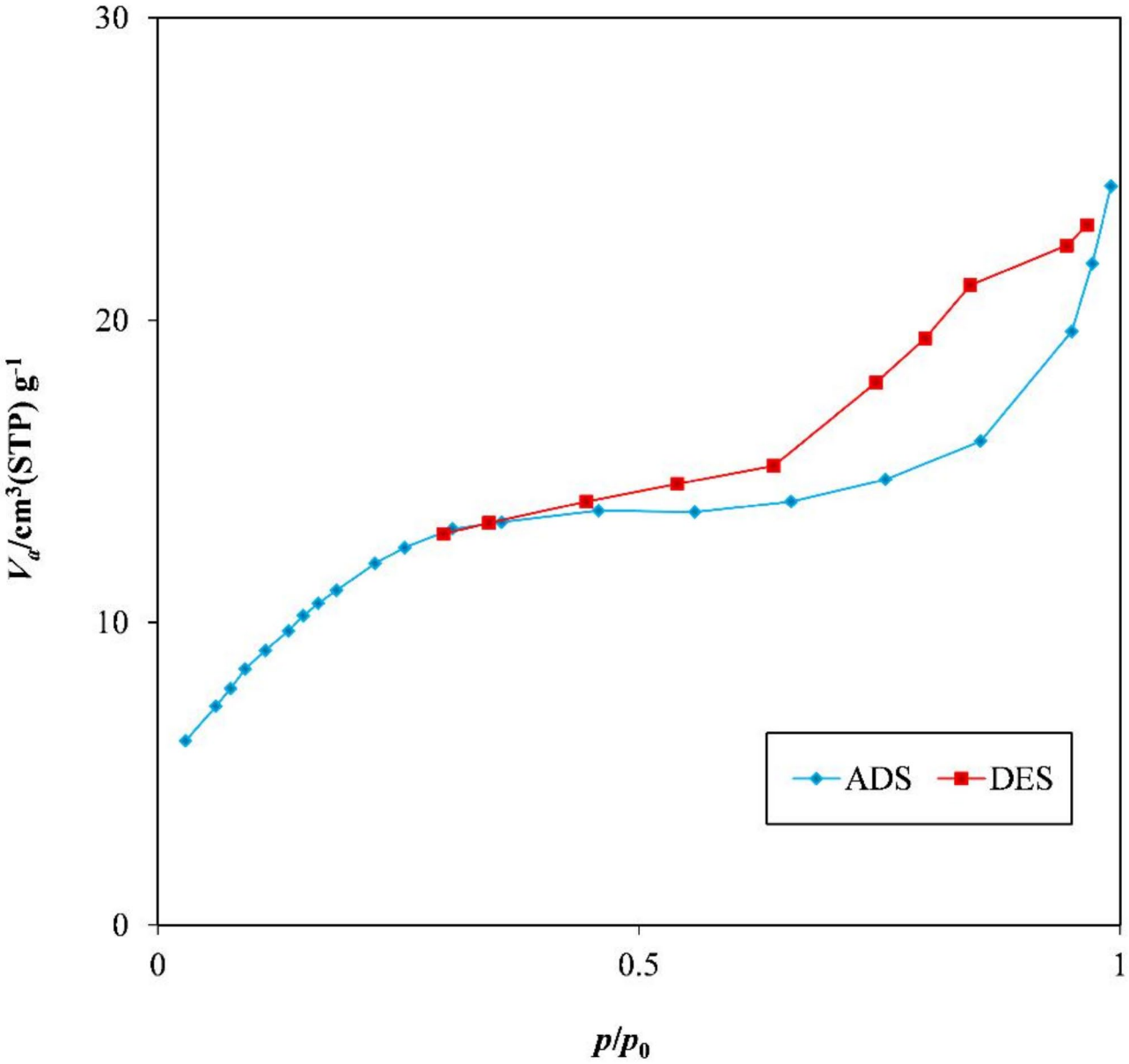

Fig. 6. The BET isotherm of the synthesized αFe_2O_3/CuO nanocomposite.

Besides, the Lack of Fit value for the final model was found to be 0.1944, which is considered insignificant. A Lack of Fit value greater than 0.05 typically suggests that the model does not provide a good fit to the experimental data, while a value below 0.05 indicates an adequate fit[39,41]. In this case, the insignificant Lack of Fit value indicates that the model provides a reliable and accurate representation of the experimental data, confirming that the statistical model is well-suited for predicting the biodiesel yield under the studied conditions. The ANOVA analysis demonstrates that both the methanol/WCO molar ratio and reaction temperature are the primary drivers of biodiesel yield, with catalyst amount also playing a significant role. The high statistical significance of these parameters, coupled with the insignificant Lack of Fit value, validates the robustness and accuracy

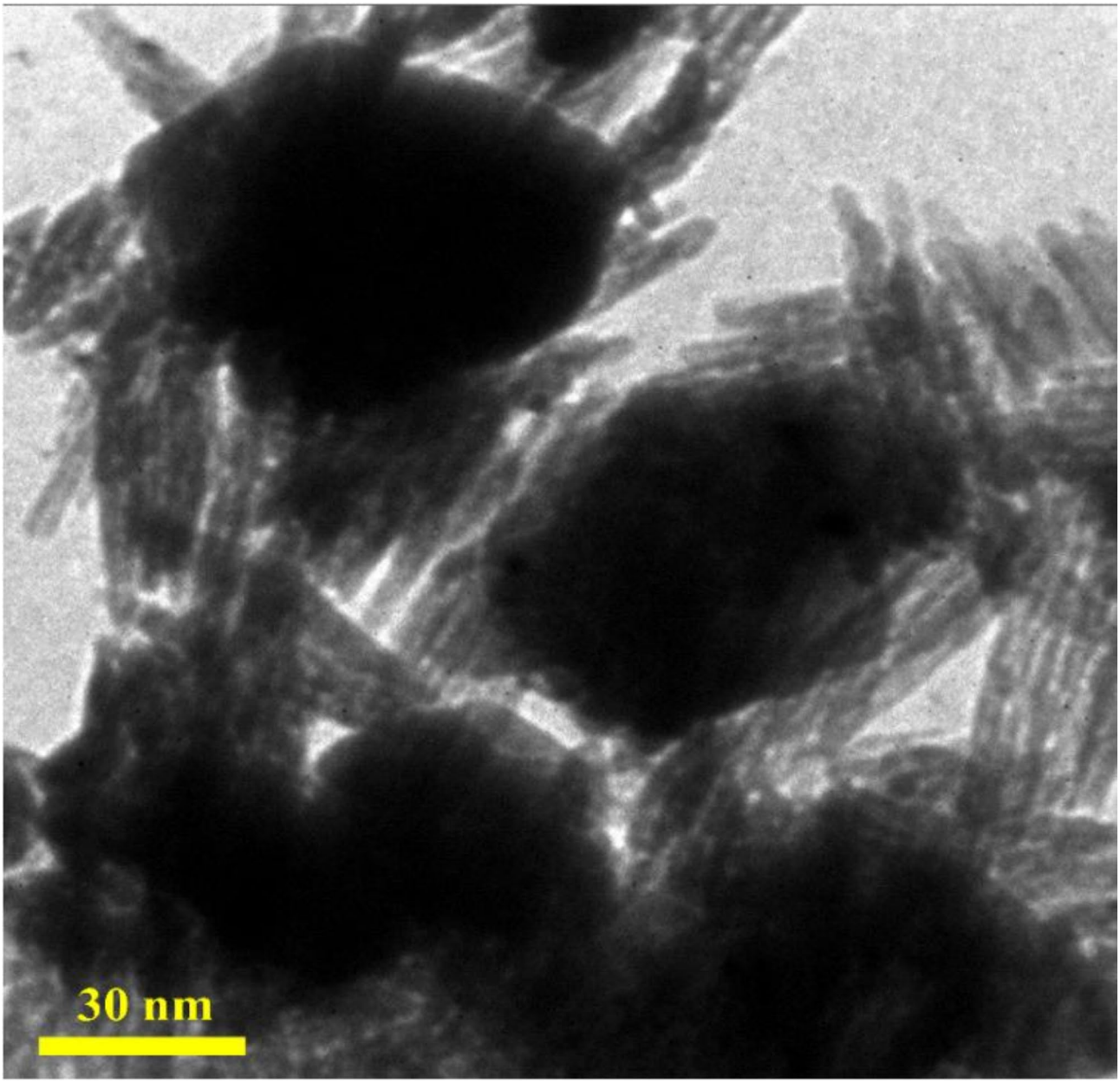

Fig. 7. TEM image for αFe_2O_3/CuO nanocatalyst synthesized by co-precipitation method.

of the model in predicting biodiesel production. Besides, to evaluate the model's reliability, several statistical parameters were examined, including the coefficient of determination (R^2), adjusted coefficient of determination (R-adj^2), and predicted coefficient (R-predictd^2), all calculated using the RSM-BBD approach[41,42]. The results showed R^2, R-adj^2, and R-predictd^2 values of 0.9994, 0.9986, and 0.9933, respectively. These high values indicate a strong correlation between the model and the experimental data, suggesting that the model accurately predicts biodiesel yield and captures the relationships between the process variables. The close agreement between R^2, R-adj^2, and R-predictd^2 further confirms the model's robustness and reliability[40,42].

The perturbation plot illustrating the effects of three quantitative parameters on biodiesel yield is presented in Fig. 8. In these plots, the response is evaluated by varying one parameter across its entire range while keeping the other variables fixed at a reference point. In Fig. 8 (a), the intersecting lines indicate an interaction between the methanol/WCO molar ratio (X_1) and the temperature (X_3). This interaction suggests that the impact of temperature on methyl ester purity varies depending on the methanol/WCO molar ratio. Consequently, precise adjustments to both temperature and the methanol/WCO molar ratio are essential to achieve optimal yield. Similarly, Fig. 8 (b) shows intersecting lines for the methanol/WCO molar ratio (X_1) and the catalyst loading (X_2), highlighting their interactive effect. This implies that the impact of one parameter on biodiesel yield depends on the value of the other[42]. This complex interaction underscores the need for careful optimization of these two parameters to maximize yield. Conversely, Fig. 8 (c) reveals non-intersecting lines for the catalyst

Run	Type	Molar ratio (mol/mol)	Catalyst dosage (wt%)	Temperature (°C)	Yield (%)
1	Center	11	2	60	93.78
2	Fact	8	2	70	70.32
3	Center	11	2	60	94.16
4	Fact	11	3	50	79.24
5	Fact	8	3	60	78.11
6	Fact	14	1	60	80.07
7	Fact	14	2	70	82.16
8	Fact	11	3	70	82.37
9	Fact	14	3	60	77.26
10	Fact	11	1	70	80.14
11	Fact	8	1	60	70.35
12	Center	11	2	60	94.27
13	Fact	14	2	50	71.68
14	Center	11	2	60	93.67
15	Fact	11	1	50	76.15
16	Fact	8	2	50	75.45
17	Center	11	2	60	94.04

Table 4. The trials designed via RSM along with biodiesel yield in different empirical circumstances.

Source	Sum of squares	df	Mean square	F-value	*p*-value
Model	1225.89	9	136.21	1280.10	< 0.0001
X_1-Molar ratio (mol/mol)	35.87	1	35.87	337.11	< 0.0001
X_2-Catalyst dosage (wt%)	13.18	1	13.18	123.90	< 0.0001
X_3-Temperature (°C)	19.44	1	19.44	182.67	< 0.0001
$X_1 \times_2$	27.93	1	27.93	262.50	< 0.0001
$X_1 \times_3$	60.92	1	60.92	572.50	< 0.0001
$X_2 \times_3$	0.1849	1	0.1849	1.74	0.2289
X_1^2	514.53	1	514.53	4835.56	< 0.0001
X_2^2	176.91	1	176.91	1662.60	< 0.0001
X_3^2	271.30	1	271.30	2549.62	< 0.0001
Residual	0.7448	7	0.1064		
Lack of fit	0.4887	3	0.1629	2.54	0.1944
Pure error	0.2561	4	0.0640		
Cor total	1226.64	16			

Table 5. Statistical assessment report ANOVA for synthesizing biodiesel from WCO via AFe_2O_3/CuO nanocomposite.

loading (X_2) and the temperature (X_3) when the methanol/WCO molar ratio is held constant. This absence of interaction suggests that changes in catalyst loading and temperature independently affect biodiesel yield, with no direct influence on each other[43].

To evaluate the model's accuracy, the normal distribution of residuals was examined. Figure 9 (a) shows the residuals' alignment with a reference line, indicating they are normally distributed. This supports the statistical validity of the model employed in the experiment[44]. Additionally, the relationship between the predicted and actual values of biodiesel yield is shown in Fig. 9 (b). The maximum predicted yield is 94.27%, while the corresponding actual experimental yield is 95.08%. This consistency highlights the reliability of the model, with the optimal process conditions being identified in experiment no. 12. Figure 9 (c) depicts the residuals plotted against the predicted biodiesel yield values. The random scatter of residuals around the zero line suggests that there is no systematic bias in the model, indicating that the residuals are independent of the predicted response variable[43,44]. This distribution confirms the robustness of the model in accurately describing the biodiesel production process[45]. Additionally, the residuals fall within a range of ± 4.82, highlighting the data's quality and consistency within the bounds of the experimental design. This tight range ensures that the model's predictions remain well-calibrated and that any observed deviations are due to random error rather than systemic issues in the model or experimental methodology[46].

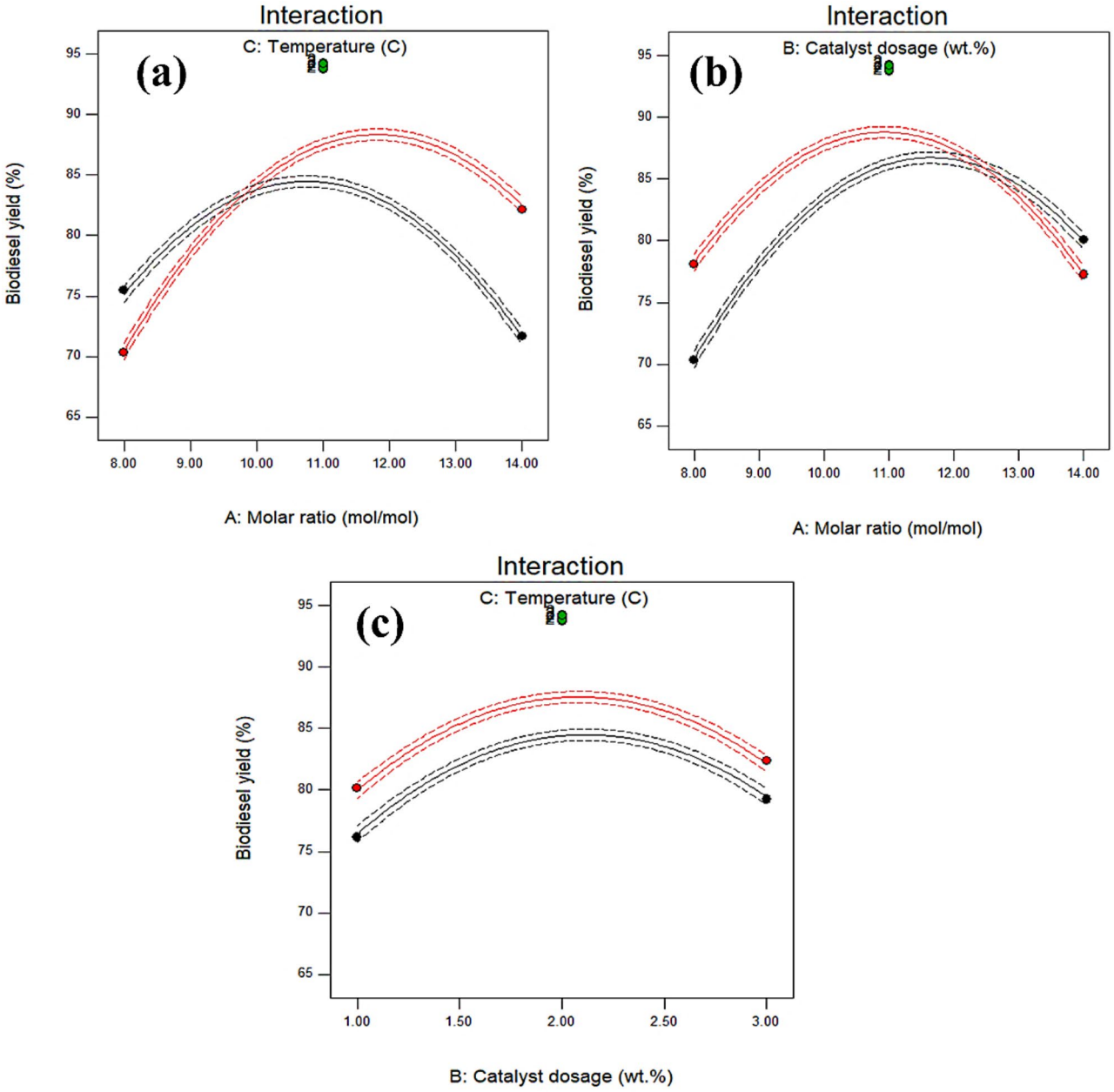

Fig. 8. Turbulence plots (**a**) Methanol/WCO molar ratio and temperature (**b**) Methanol/WCO molar ratio and catalyst loading (**c**) Catalyst loading and temperature.

Vital variables on the biodiesel generation via αFe2O3/CuO

Figure 10 illustrates the interaction effects of key parameters on biodiesel yield during the transesterification process using αFe_2O_3/CuO nanocomposite. Figure 10 (a) reveals the interaction between catalyst loading (X_2) and the methanol/WCO molar ratio (X_1) on biodiesel yield at a constant temperature of 60 °C and reaction time of 3 h. The outcomes demonstrate that biodiesel yield improved initially with catalyst loading up to 2 wt%, after which it decreased at 3 wt%. A similar trend was observed for the methanol/WCO molar ratio, where FAME yield increased at a molar ratio of 11:1 but decreased when the ratio exceeded 14:1. The initial increase in both catalyst loading and methanol/WCO molar ratio enhances the number of active sites, thereby improving the interaction between the reactant and the catalyst, leading to higher biodiesel yield[46,47]. However, when catalyst loading exceeded 2 wt%, the yield decreased, likely due to emulsion formation and increased viscosity, which hinder phase separation. Similarly, very low or very high methanol/WCO ratios resulted in suboptimal conditions. Insufficient methanol fails to drive the reaction, while excessive methanol hinders glycerol separation and interferes with the catalyst's active sites[48]. These findings emphasize the need to optimize both nanocatalyst loading and the methanol/WCO molar ratio for efficient transesterification. Figure 10 (b) presents the interaction between catalyst loading (X_2) and temperature (X_3), with the methanol/WCO molar ratio fixed at 11:1 and reaction time set at 3 h. The three-dimensional plot reveals that FAME yield increases

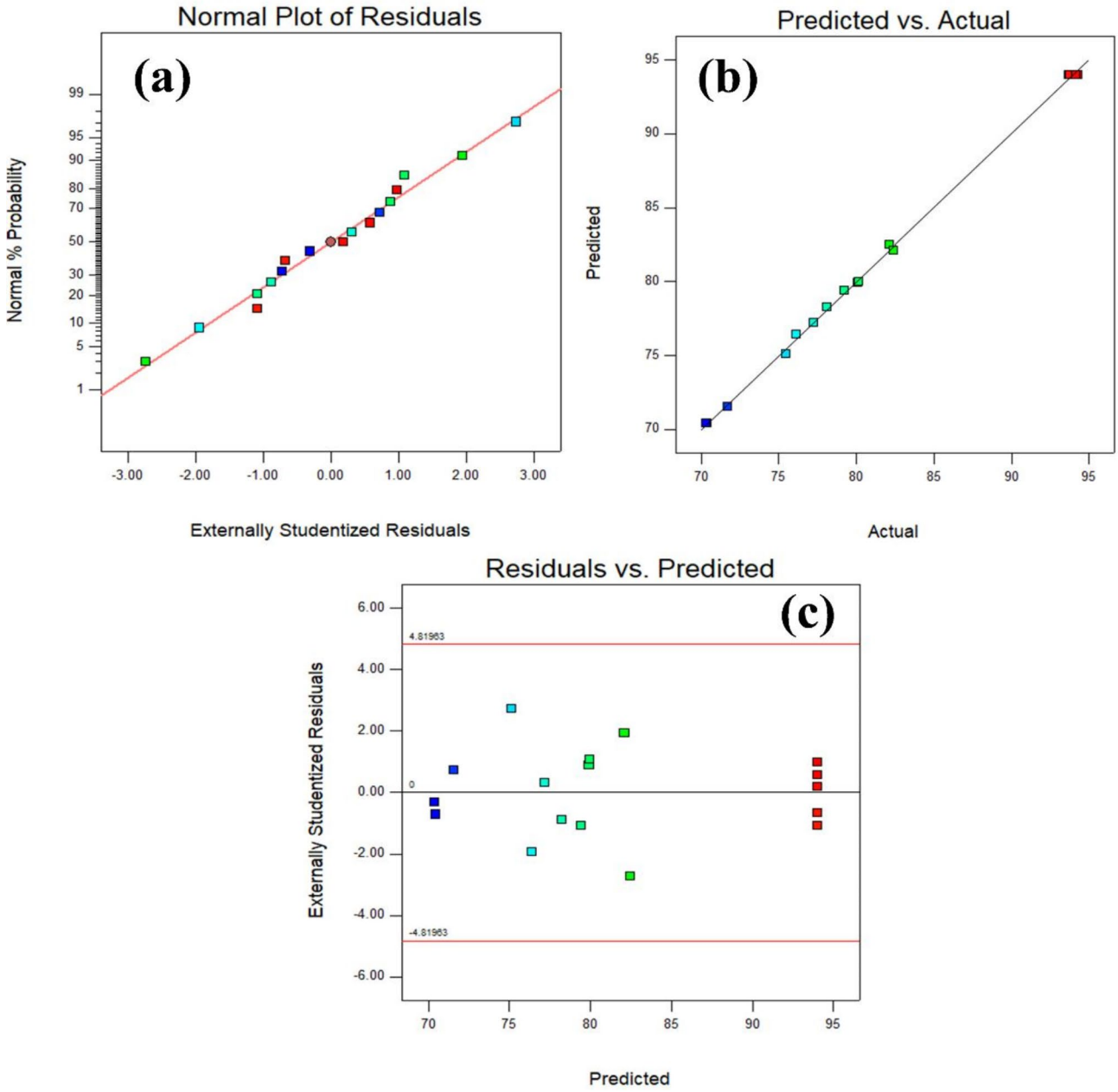

Fig. 9. (**a**) Normal probability distribution of residuals (**b**) Experimental predicted values (**c**) Random plot of residuals in terms of efficiency fitting values for biodiesel synthesis from WCO employing αFe_2O_3/CuO nanocomposite.

with both temperature and catalyst loading, but shows a slight decrease at 70 °C and 3 wt% catalyst. This reduction is attributed to methanol evaporation, as its boiling point is 64.9 °C, which reduces the contact time between methanol and oil, ultimately lowering reaction efficiency[48]. Temperature plays a crucial role in biodiesel production, and for catalysts like αFe_2O_3/CuO, an optimal temperature range of 50 to 65 °C is typically required for efficient transesterification. Figure 10 (c) illustrates the combined effect of the methanol/WCO molar ratio (X_1) and temperature (X_3) on biodiesel yield, with catalyst loading fixed at 2 wt% and reaction time at 3 h. The results indicate that biodiesel purity boosts with both temperature and methanol/WCO molar ratio up to certain levels, after which the yield decreases. Increasing the temperature enhances the kinetic energy of the molecules, leading to faster reaction rates and improved conversion of triglycerides to methyl esters. Moreover, higher temperatures reduce viscosity, improving the mixing of reactants and facilitating the reaction's progress toward completion[46,47]. On the other hand, methanol acts as a reactant and solvent, shifting the equilibrium toward product formation when used in excess. A higher molar ratio ensures sufficient methanol molecules are available to interact with triglycerides, promoting complete transesterification and minimizing unreacted glycerides[48,49]. However, an excessively high ratio may lead to challenges in methanol recovery and diminish yield. This decrease

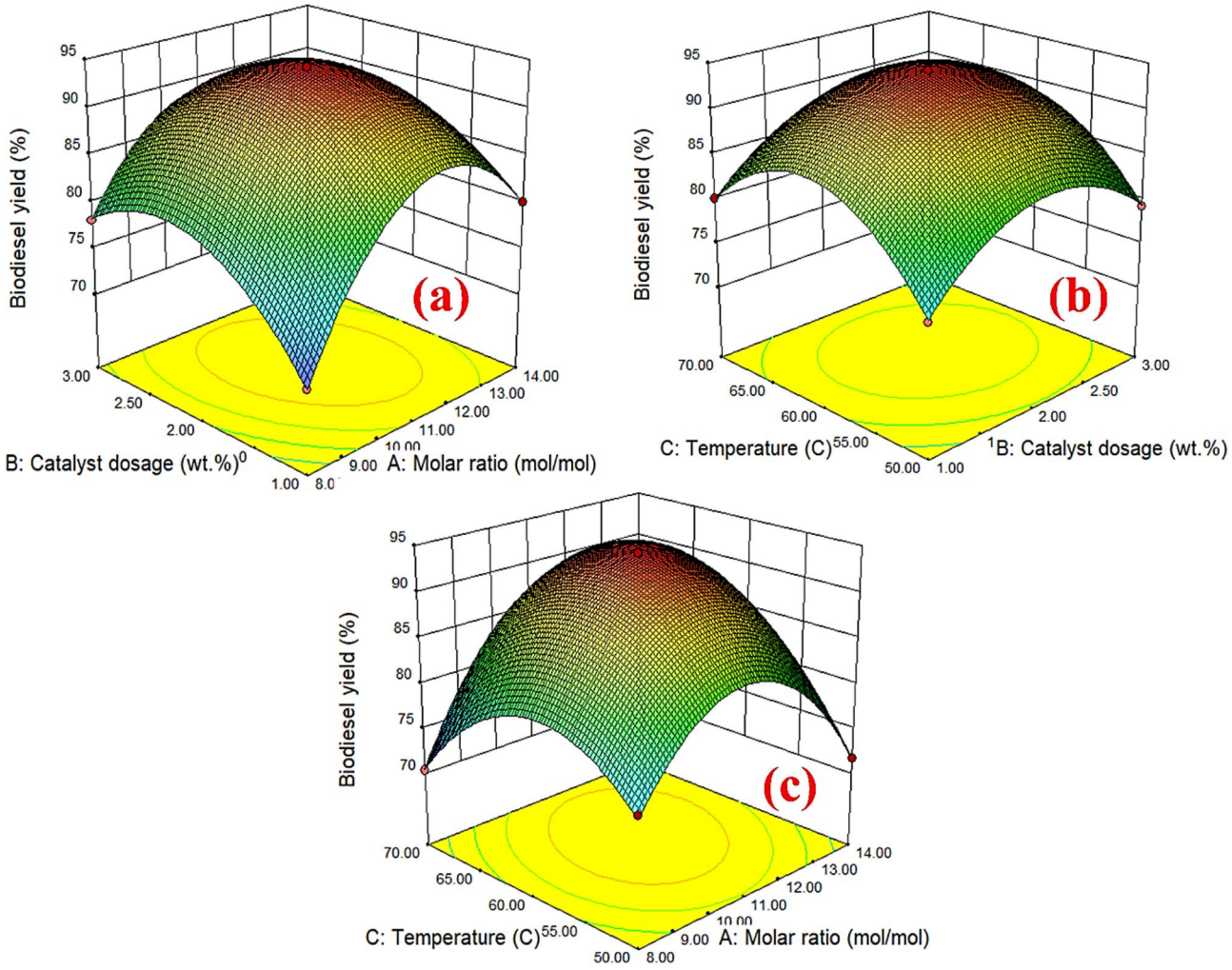

Fig. 10. Response surface plots of the interactions between (**a**) molar ratio and catalyst amount (**b**) temperature and catalyst amount (**c**) temperature and molar ratio on biodiesel yield from WCO employing αFe_2O_3/CuO nanocatalyst.

is observed when the methanol/WCO molar ratio is low (8:1) and temperature exceeds 65 °C, causing methanol evaporation and reducing the reaction's effectiveness. The optimal biodiesel yield was achieved with a methanol/WCO molar ratio of 11:1 and a temperature near 65 °C. Overall, the analysis demonstrates that both catalyst loading and methanol/WCO molar ratio significantly affect biodiesel yield, with specific interactions between these parameters and temperature influencing overall performance[47]. Besides, proper optimization of these parameters is essential for achieving high biodiesel yields, ensuring efficient transesterification, and minimizing potential issues such as emulsion formation and methanol evaporation[46,48].

Optimization by BBD methodology

Figure 11 illustrates the optimization of reaction parameters using RSM in combination with BBD, a statistical technique for modeling and analyzing the effects of multiple variables. The aim of the study was to assess the optimal circumstances for maximizing biodiesel production efficiency. Based on the results presented in the figure, the optimal reaction parameters were found to be a methanol/WCO ratio of 11:1 mol/mol, a nanocatalyst loading of 2 wt%, and a reaction temperature of 60 °C. Under these conditions, the biodiesel production efficiency reached a peak of 94.27%, representing the highest efficiency observed in the experimental analysis. To confirm the model's accuracy and reproducibility, the optimal conditions were tested in three independent repetitions[47]. The average biodiesel efficiency from these repetitions was 93.92%, closely aligning with the predicted efficiency. This slight deviation occurs due to slight variations in experimental conditions or inherent uncertainties in the model's predictions. This agreement between experimental and predicted values demonstrates the reliability and accuracy of the model. Thus, the optimization model developed using RSM and BBD serves as a robust tool for predicting biodiesel production efficiency under varying experimental conditions. The consistency of these results further emphasizes the model's potential for scaling up biodiesel generation processes[48,49].

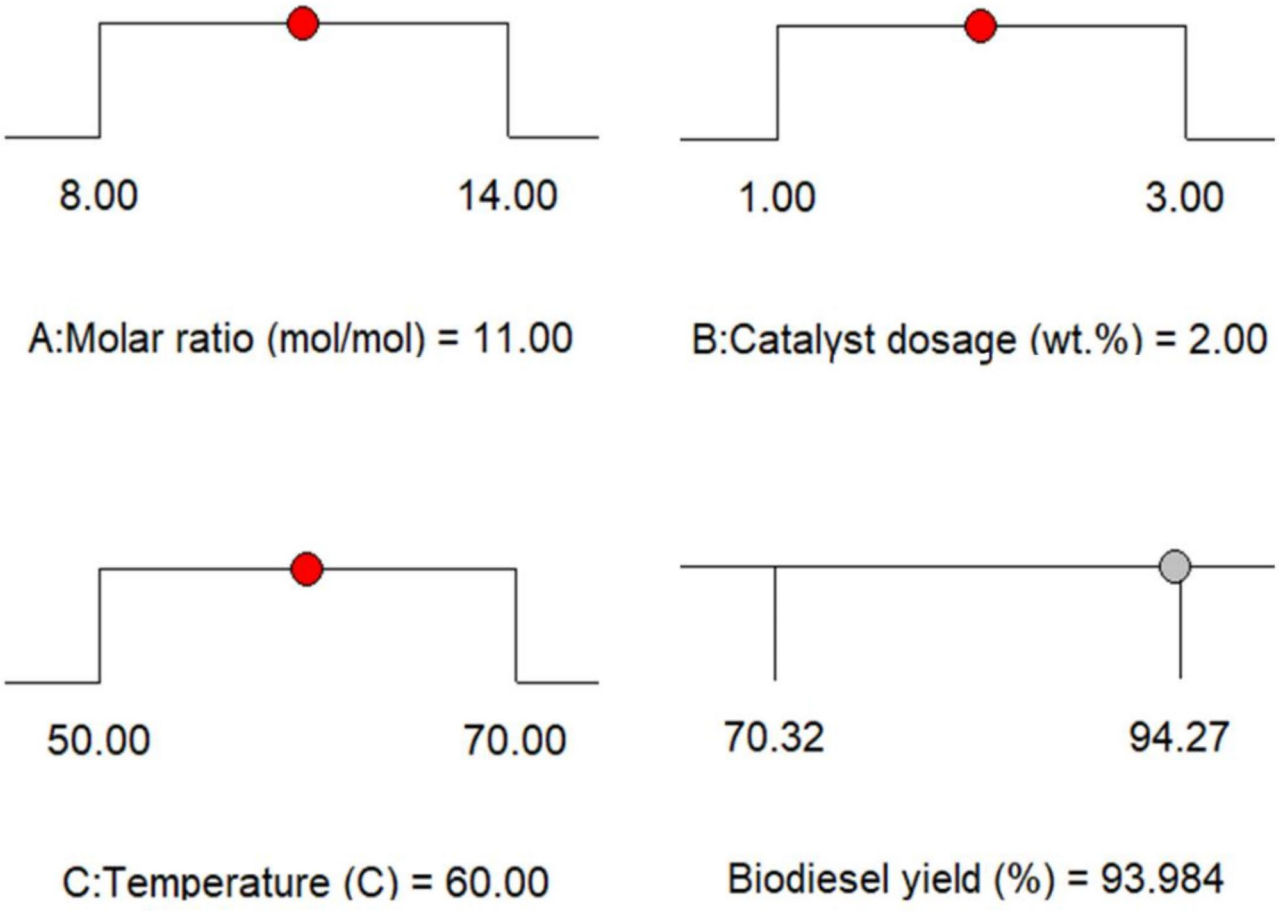

Fig. 11. Optimum conditions for generated methyl ester yield employing αFe_2O_3/CuO.

Stability of αFe2O3/CuO nanocatalyst

The reusability of heterogeneous catalysts, particularly the αFe_2O_3/CuO nanocatalyst, plays a vital role in assessing its stability and overall performance in catalytic applications[50]. This study thoroughly examined the performance of the αFe_2O_3/CuO nanocatalyst in biodiesel production via transesterification. The optimal reaction conditions were determined to be a methanol/WCO molar proportion of 9:1, a catalyst loading of 2 wt%, a constant reaction time of 3 h, and a reaction temperature of 60 °C. After each reaction cycle, the catalyst was thoroughly washed multiple times with methanol to remove adsorbed glycerol and other impurities. This step was then followed by drying the catalyst at 100 °C for 24 h to ensure proper activation before reuse in subsequent cycles. As shown in Fig. 12, the biodiesel yield was 90.27% during the first cycle. However, with each subsequent reuse, the yield gradually decreased. By the seventh cycle, the yield had dropped to 86.16%, indicating a reduction in catalytic activity over time. This decrease in activity can be attributed to various factors. One possible cause is inadequate washing of the catalyst between cycles, which may lead to the degradation of active sites and a decrease in catalytic efficiency[15,49]. Additionally, the accumulation of triglycerides and glycerol on the catalyst's surface can obstruct active sites and pores, further hindering its performance[50]. These findings highlight the importance of optimal washing and regeneration conditions to preserve the nanocatalyst's activity and stability during recycling[49,51]. Overall, while the αFe_2O_3/CuO nanocatalyst displayed relatively good stability over multiple cycles, its performance gradually decreased due to catalyst deactivation and the blocking of active sites. To maintain its activity and maximize reusability in biodiesel production, it is essential to implement proper maintenance and optimize regeneration techniques. Besides, the permissible level of catalyst leaching in the produced biodiesel was evaluated using inductively coupled plasma mass spectrometry (ICP-MS). The analysis indicated a leaching value of 2.1 mg/kg, which complies with the acceptable range specified by the EN 14,214 standard.

Figure 13 reveals a comparison of images of fresh and used nanocatalysts. The surface of the fresh αFe_2O_3/CuO nanocatalyst demonstrates a well-defined morphology, with smooth, well-dispersed nanoparticles that are likely spherical or irregular in shape, exhibiting a uniform size distribution. This suggests a high degree of homogeneity in the fresh catalyst. The surface remains clean, with minimal aggregation or structural degradation. The catalyst is expected to have high porosity and surface area, characteristics typical for catalysts optimized for biodiesel production[48,49]. In contrast, the SEM image of the utilized nanocatalyst reveals significant changes, including particle aggregation or enlargement, which likely results from sintering or coalescence due to high temperatures or chemical interactions during the catalytic process. The surface morphology may show

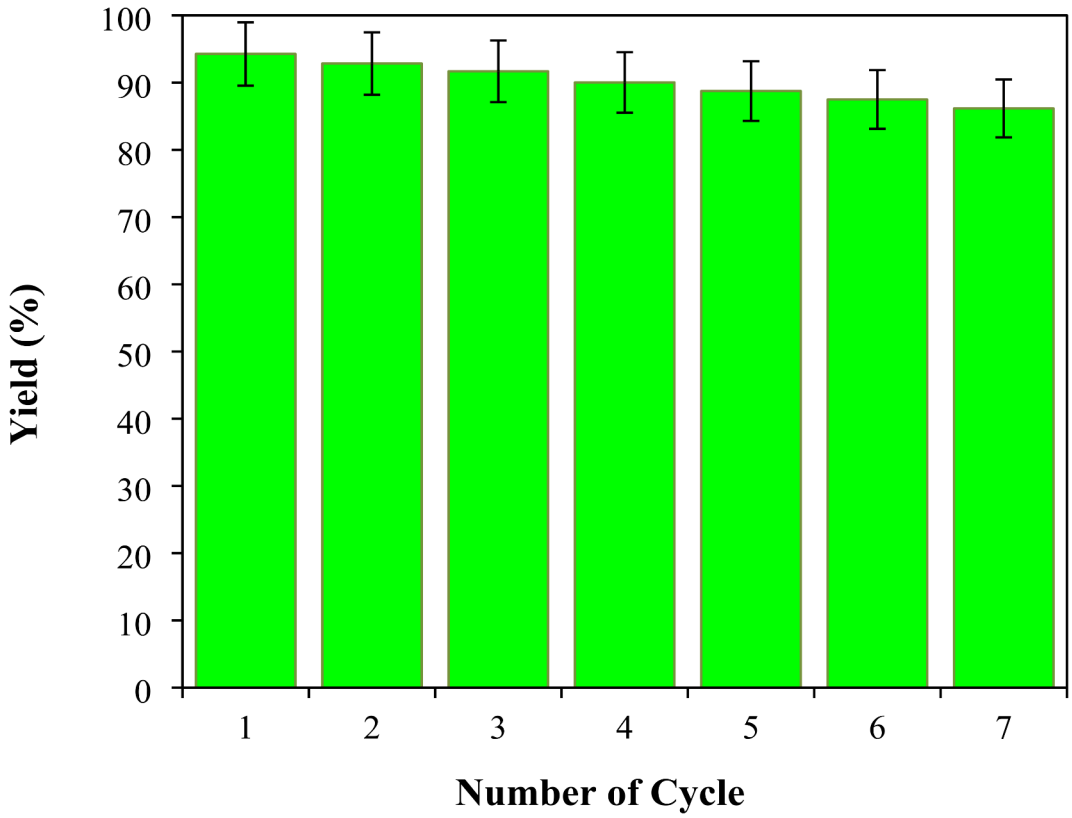

Fig. 12. Stability assessment of αFe_2O_3/CuO nanocatalyst in seven rounds.

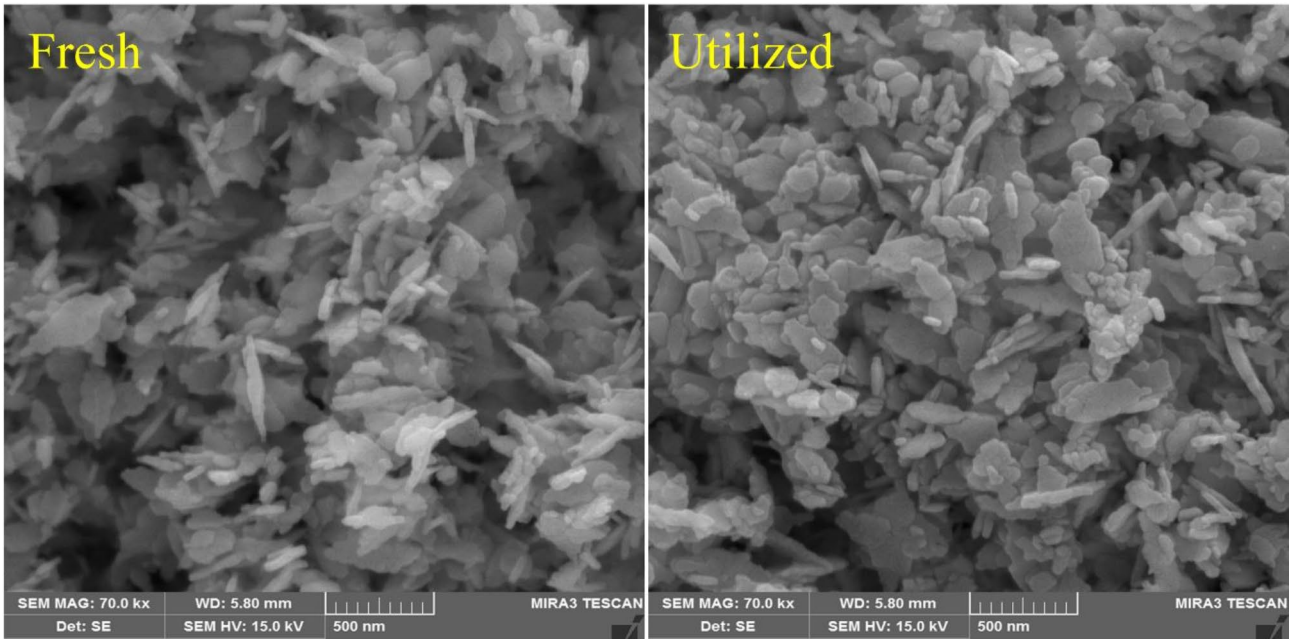

Fig. 13. SEM images of fresh and utilized for αFe_2O_3/CuO nanocatalyst.

reduced porosity, possibly leading to pore blockage, which could compromise catalytic efficiency. The surface roughness might also increase, possibly due to the deposition of reaction by-products or hydrocarbon residues[50]. Additionally, there could be signs of catalyst deactivation, such as changes in structural integrity or uneven particle distribution, indicating reduced catalytic activity after multiple cycles[51].

In the present study, the αFe_2O_3/CuO nanocatalyst exhibited the highest biodiesel production efficiency (94.27%) despite utilizing a relatively low catalyst loading of 2 wt%. As illustrated in Table 6, other studies employing $MgO/MgAl_{0.4}Fe_{1.6}O_{0.4}$ and $MgO/MgFe_2O_4$ catalysts utilized higher catalyst loadings of 14% and 12 wt%, respectively. This suggests that the incorporation of copper oxide nanoparticles into the αFe_2O_3/CuO catalyst may significantly enhance its catalytic activity, leading to higher biodiesel yields even at a lower catalyst loading. The use of a lower catalyst percentage not only enhances process efficiency but also reduces production costs, thereby improving the economic feasibility of the process[51,52]. Moreover, catalysts with lower loadings may offer better selectivity and minimize side reactions, further optimizing performance. The methanol/WCO molar ratio employed in this study (11:1) falls between those used in other studies (12:1 and 9:1), indicating that this ratio is well-optimized for the reaction conditions. Maintaining this optimal ratio ensures that the methanol loading remains sufficiently high to facilitate the transesterification reaction, thereby enhancing biodiesel production efficiency[52]. Additionally, the use of waste oil, specifically sunflower frying waste oil, distinguishes this study from others that typically utilize pure sunflower or canola oils for biodiesel production. Utilizing waste oil not only reduces raw material costs but also promotes environmental sustainability by repurposing waste materials for biodiesel synthesis. The reaction time of 3 h and reaction temperature of 60 °C were identified as optimal conditions in this study when compared to other experiments. The 3-hour reaction time ensures that the transesterification process is completed efficiently, while the 60 °C reaction temperature supports effective catalyst activity without compromising the stability of either the catalyst or the reaction. The mention of 3 h reaction time as an optimal parameter corresponds to the fixed reaction time established from preliminary experiments conducted prior to designing the Box-Behnken optimization experiments. Although reaction time was not considered a variable in the optimization model, it was determined based on previous studies and experimental trials, where equilibrium was consistently reached within 3 h under the selected conditions. These optimized conditions contribute to both the efficiency and sustainability of the biodiesel production process, underscoring the significance of precise reaction parameters in achieving high yields.

Characterization of WCO-derived biodiesel

The FTIR spectra for WCO and WCO-derived biodiesel, illustrated in Fig. 14, reveal distinct differences that confirm the successful transesterification process. One key observation is the absence of the absorption band in the 3000–3500 cm^{-1} range, which typically corresponds to the bending vibration of the -OH group[55]. This absence reveals that the methyl ester is free from unreacted methanol, suggesting that the transesterification process was completed without any residual alcohol or water. Prominent peaks at 2918 cm^{-1} and 2932 cm^{-1} correspond to the asymmetric and symmetric stretching vibrations of the aliphatic C-H bonds in the CH_2 and CH_3 groups, respectively[55,56]. These peaks are characteristic of fatty acid methyl esters (FAMEs) found in biodiesel, signaling the successful conversion of triglycerides into methyl esters during the transesterification reaction. Additionally, a C = O stretching vibration appears at 1697 cm^{-1} in the WCO sample, indicating the presence of glycerides (glycerin esters) in the original oil[54,57]. In contrast, the WCO-derived biodiesel exhibits a shift in the C = O stretching vibration to approximately 1739 cm^{-1}, confirming the formation of methyl esters and the successful transesterification process[58]. This shift indicates that the αFe_2O_3/CuO nanocatalyst has successfully facilitated the conversion of WCO into biodiesel. The observed change in the carbonyl stretching vibration provides clear evidence of the transesterification process, highlighting the catalyst's effectiveness in transforming glycerides into methyl esters.

H-NMR assess was employed to confirm the chemical features of WCO and the biodiesel produced utilizing the αFe_2O_3/CuO nanocatalyst. The H-NMR spectra, demonstrated in Fig. 15, reveal several distinct peaks in both the WCO and its biodiesel derivative. Key peaks observed include 0.93, 1.30, 1.66, 2.11, 2.38, 2.79, 4.32, and 5.37 ppm, which correspond to various proton environments within the molecules[55,56]. Specifically: The signals at 0.93 and 1.30 ppm are attributed to the CH_2 groups. The peak at 1.66 ppm corresponds to β-CH_2. Peaks at 2.11 and 2.38 ppm are associated with the = CH-CH_2 and α CH_2 groups, respectively[15,57]. The 2.79 ppm peak is linked to the –CH_2-CH_2-CH = group. The peaks at 4.32 and 5.37 ppm correspond to CH_2 and –CH = CH- groups, respectively. After the transesterification of WCO into biodiesel using the αFe_2O_3/CuO nanocatalyst, the H-NMR spectra revealed subtle shifts in the intensities and positions of some peaks. Moreover, the peaks

Refs.	Yield (%)	Reaction parameters	Feedstock	Catalyst
[52]	93.2	12:1 CH_3OH/oil proportion, 14 wt% catalyst dosage, reaction temperature of 55 °C for 1 h	Sunflower	$MgO/MgAl_{0.4}Fe_{1.6}O_{0.4}$
[53]	91.2	9:1 CH_3OH/oil molar ratio, catalyst dosage of 12 wt%, reaction temperature of 65 °C for 4 h.	Sunflower	$MgO/MgFe_2O_4$
[15]	92.72	12:1 CH_3OH/oil molar ratio, 2.53 wt% catalyst dosage, 65 °C reaction temperature for 0.5 h	Sunflower	αFe_2O_3/ZnO
[54]	97.42	Temperature 62.36 °C, CH_3OH/DWSO proportion 11:12, nanocatalyst dosage of 2.76 wt%, time 2.85 h	Dairy waste oil	CuO/RHA
[41]	98.04	Temperature 65 °C, CH_3OH/DWSO proportion 12.75:1, nanocatalyst dosage of 1.53 wt%, time 7.17 min	Annona squamosa L. seed oil	Co_3O_4@rGO
[45]	97.81	Temperature 65 °C, CH_3OH/DWSO proportion 11.24:1, nanocatalyst dosage of 2.41 wt%, time 36.62 min	Dairy waste oil	AC@ZnO/NiO
[5]		Temperature 65 °C, CH_3OH/Castor oil proportion 18:1, nanocatalyst dosage of 3 wt%, time 120 min	Castor oil	Rice husk ash/CuO/K_2CO_3
This research	94.27	Temperature 62.36 °C, CH_3OH/WCO proportion 11:1, nanocatalyst dosage of 2 wt%, temperature 60 °C for 3 h	Waste cooking oil	αFe_2O_3/CuO

Table 6. Summarizing the activity of AFe_2O_3/CuO nanocatalyst with other catalysts in transesterification reaction.

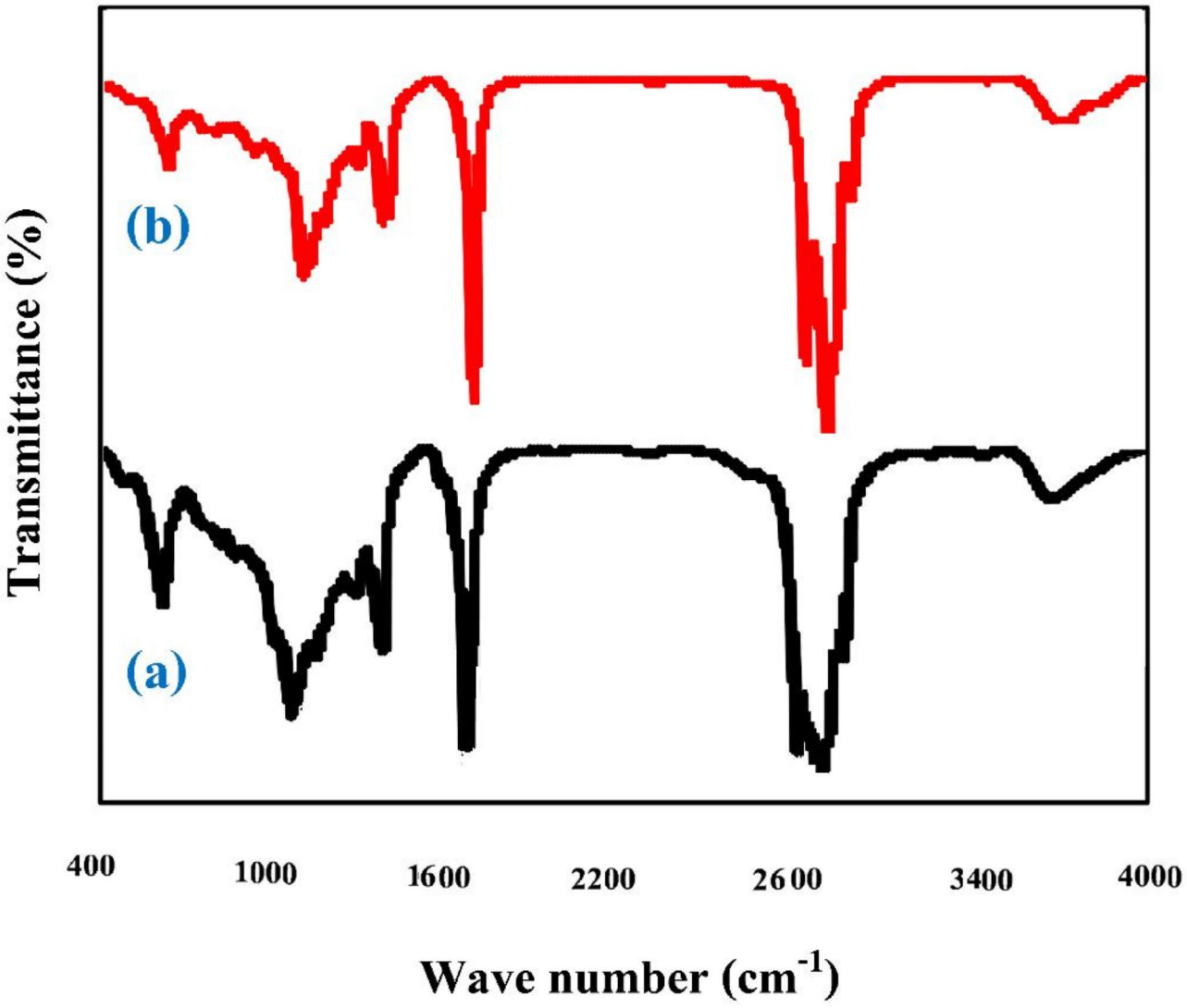

Fig. 14. FTIR of WCO (**a**) and its conversion to WCO ME (**b**).

at 1.30 ppm and 2.36 ppm in the WCO spectrum shifted to 1.37 ppm and 2.29 ppm in the biodiesel spectrum, respectively[58]. These shifts suggest minor changes in the molecular environment owing to the transesterification reaction. A new peak appeared at 3.71 ppm in the biodiesel spectrum, corresponding to methoxy protons ($-OCH_3$), a critical indicator of successful conversion from WCO to biodiesel and confirming the formation of methyl esters[56,59]. These spectral changes affirm the successful synthesis of biodiesel from WCO and demonstrate the effectiveness of the $\alpha Fe_2O_3/CuO$ nanocatalyst in the transesterification reaction.

Mechanism

The stepwise mechanism of biodiesel production from WCO utilizing $\alpha Fe_2O_3/CuO$ nanocatalyst is depicted in Fig. 16. Step 1 contains the adsorption of reactants onto the catalyst surface. The first step in the transesterification process involves the adsorption of triglycerides, the primary component of WCO, and methanol onto the active sites of the $\alpha Fe_2O_3/CuO$ nanocatalyst. The catalyst's high surface area and well-dispersed active sites facilitate the efficient interaction of the reactant molecules with the catalyst surface. This adsorption is critical for ensuring the proximity of reactants and creating a conducive environment for subsequent chemical transformations[15,46]. Besides, step 2 possesses activation of methanol. Upon adsorption, methanol undergoes activation on the catalyst surface. The $\alpha Fe_2O_3/CuO$ nanocatalyst plays a dual role, providing Lewis acid and base sites that facilitate the dissociation of methanol into highly reactive methoxide ions (CH_3O^-). The generation of these nucleophilic species is a key step in initiating the transesterification reaction[55]. Moreover, Step 3 includes nucleophilic attack of methoxide ions. The methoxide ions generated in the previous step attack the carbonyl carbon atoms of the triglyceride molecules. This nucleophilic substitution reaction breaks the ester bonds in the triglycerides, leading to the formation of diglycerides and methyl esters[15,59]. Further, step 4 contains progressive breakdown of intermediates. The diglycerides formed in the previous step undergo further reactions with methoxide ions. This step leads to the sequential breakdown of diglycerides and monoglycerides, ultimately producing glycerol as a

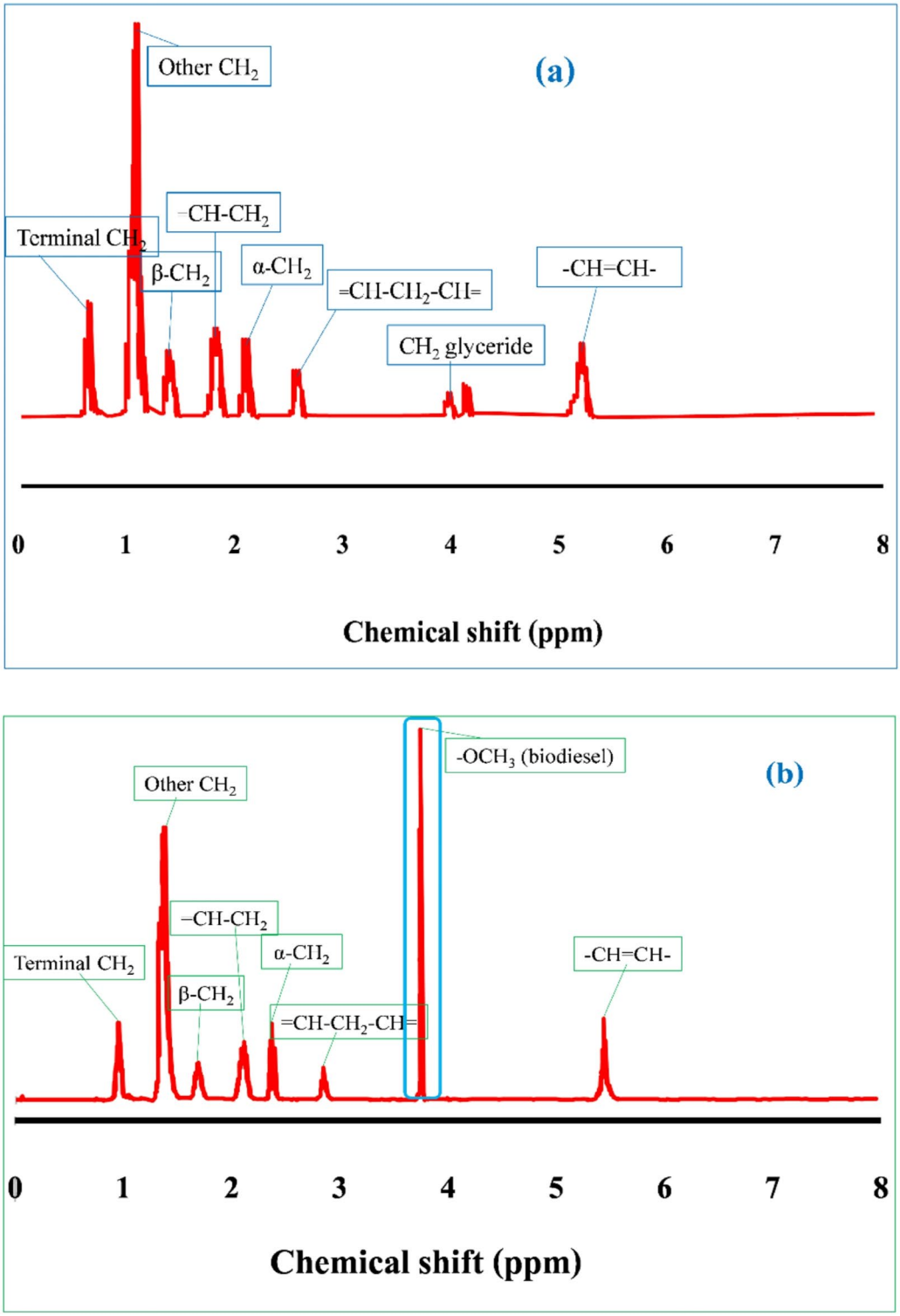

Fig. 15. H^1NMR of WCO (**a**) and its biodiesel (**b**).

by-product and additional methyl esters as the main product[59]. Finally, step 5 encloses desorption of products and regeneration of active sites. The biodiesel and glycerol are desorbed from the catalyst surface, leaving the active sites free for subsequent cycles of reaction. The structural stability and reusability of the αFe_2O_3/CuO nanocatalyst ensure its consistent performance over multiple reaction cycles[55,59]. This stepwise mechanism underscores the efficiency of the αFe_2O_3/CuO nanocatalyst in facilitating biodiesel production through enhanced adsorption, activation, and catalytic conversion processes.

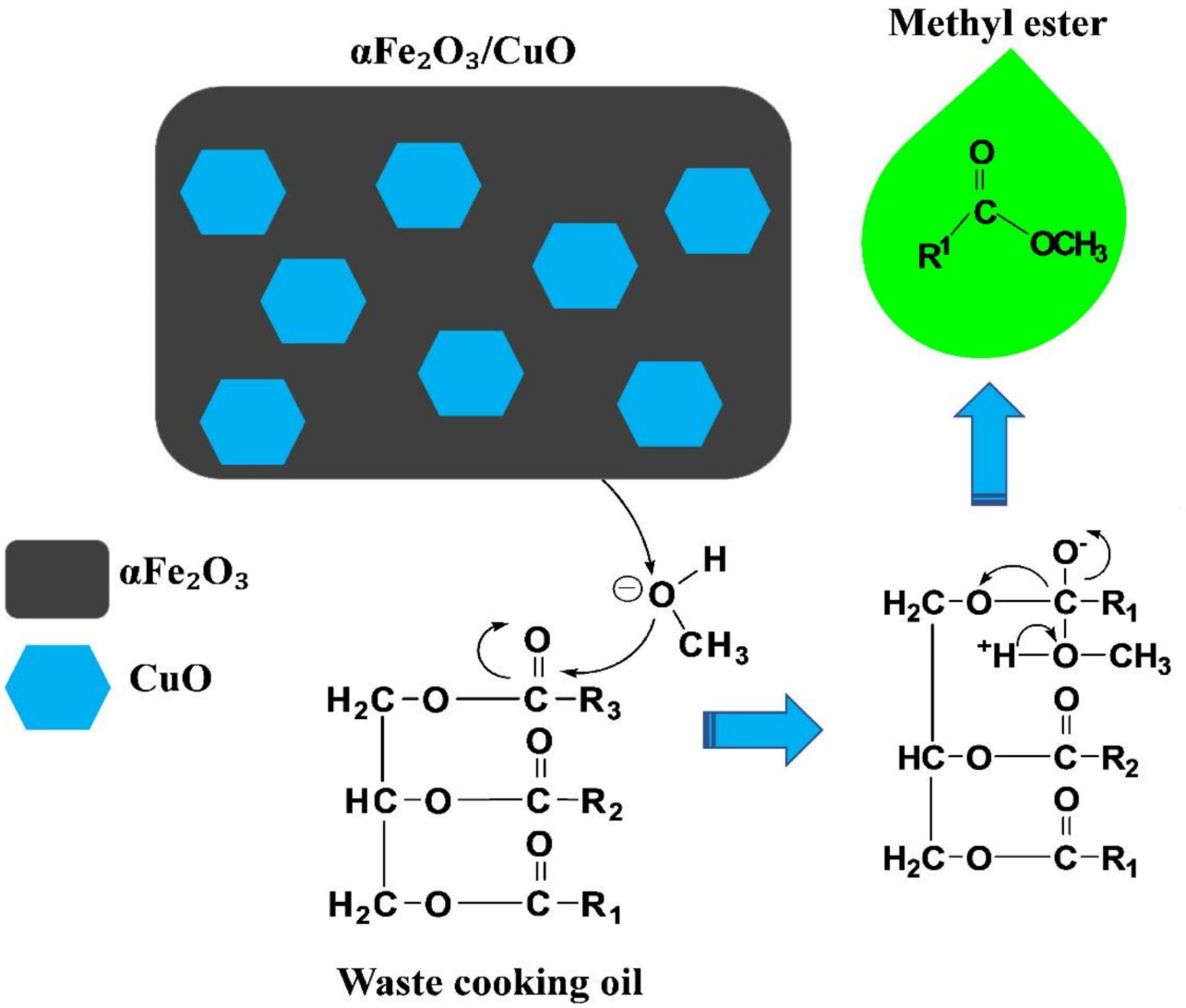

Fig. 16. Mechanism of $\alpha Fe_2O_3/CuO$ biodiesel generation.

Property	Quantity	ASTMD6751	ASTM
Acid number (mg/g KOH)	0.29	< 0.5	D664
Viscosity ($mm^2\ s^{-1}$ @ 40 °C)	4.49	1.9–6.0	D445
Density (kg/m^3@ 15 °C)	878	No specification	D976
Flash point (°C)	165	130 >	D6751
Pour point (°C)	2	− 15 to + 10	D97
Water content (mg/l)	203	< 500	D95
Cetane number	52	47 >	D613

Table 7. Features of generated biodiesel by employing AFe_2O_3/CuO nanocatalyst.

Features of WCO-derived biodiesel

To evaluate the fuel quality of WCOME synthesized from WCO, its physical and chemical features were determined and compared with ASTM criteria, as summarized in Table 7. The WCO exhibited a high density of 924 kg/m^3 and a viscosity of 39.43 cSt, both of which negatively impact fuel atomization in diesel engines. Elevated viscosity disrupts fuel spray patterns, causes incomplete combustion, diminished engine performance, and raised exhaust emissions[55]. However, these challenges were effectively addressed through the transesterification process. Following treatment, the density of WCOME was reduced to 878 kg/m^3, while its viscosity significantly decreased to 4.49 $mm^2\ s^{-1}$, aligning well with ASTM biodiesel standards. These improvements facilitate superior atomization and enhance combustion efficiency[54]. Moreover, WCOME exhibited a flashpoint of 165 °C,

Component	Formula	Amount (%)
Myristic acid	C14:0	1.57
Palmitic acid	C16:0	11.84
Stearic acid	C18:0	5.73
Oleic acid	C18:1	42.55
Linoleic acid	C18:2	35.61
Linolenic acid	C18:3	2.70

Table 8. Results obtained from GC-Mass analysis for the produced biodiesel.

approximately three times higher than that of conventional petrodiesel. This elevated flashpoint enhances safety during storage and transportation by reducing the risk of accidental ignition, a critical advantage in industrial and commercial applications that require stringent safety measures[58,59]. Water content is another key parameter in biodiesel, as it affects fuel stability and engine compatibility. Excess water can lead to free fatty acid formation, corrosion of engine components, microbial growth during storage, sedimentation, and precipitation[59]. In this study, the water content of WCOME was effectively controlled, measuring 203 mg/L well below the ASTM limit of 500 mg/L. This ensures the biodiesel's long-term stability and usability without compromising engine durability or performance. The acid value of biodiesel, indicative of its free fatty acid content, was also significantly reduced through transesterification. The acid value of WCOME decreased to 0.29 mg KOH/g, a substantial improvement compared to untreated WCO. This reduction highlights the efficiency of the transesterification process and the effectiveness of the catalyst, resulting in a refined biodiesel product with minimal risk of engine corrosion and fuel degradation. The cetane number, a critical indicator of fuel ignition quality, was determined to be 52 for WCOME, reflecting excellent compatibility with diesel engine standards and efficient combustion properties[55]. Higher cetane numbers, influenced by molecular structure (longer carbon chains increase the cetane number, while higher unsaturation reduces it), signify superior ignition performance. The achieved cetane number confirms WCOME's suitability for practical diesel engine applications. Conclusively, the transformation of raw waste oil into high-quality biodiesel through transesterification is evident[59]. Improvements in density, viscosity, flashpoint, water content, acid value, and cetane number demonstrate that WCOME not only meets ASTM standards but also offers enhanced safety, performance, and environmental advantages.

Besides, the optimized biodiesel was further characterized using gas chromatography-mass spectrometry (GC-MS), with the results summarized in Table 8. The analysis indicated that the biodiesel produced from WCO contained a diverse composition of FAMEs with carbon chain lengths ranging from C14 to C18. Among the identified fatty acids, oleic acid (C18:1) and linoleic acid (C18:2) were predominant, comprising 42.55% and 35.61%, respectively. These unsaturated fatty acids positively influence biodiesel properties, notably enhancing cold flow characteristics and oxidative stability. Minor fractions of myristic acid (C14:0) and linolenic acid (C18:3) were also detected, accounting for 1.57% and 2.70%, respectively. Additionally, saturated fatty acids such as palmitic acid (C16:0) and stearic acid (C18:0) were present at 11.84% and 5.73%, respectively.

Conclusion

In this study, an αFe_2O_3/CuO nanocatalyst was synthesized via the co-precipitation method for biodiesel production from restaurant waste oil. The nanocatalyst's physical and chemical properties were characterized using XRD, EDS, FTIR, SEM, TEM, and BET analyses. The nanoparticles exhibited a pore size of 1.21 nm and a BET surface area of 334.45 m^2/g. The results indicated that parameters such as reaction temperature, methanol/WCO molar ratio, reaction time, and catalyst loading significantly impacted the transesterification of restaurant waste oil into methyl ester. Optimization of biodiesel production parameters was conducted using response surface methodology (RSM) with a Box-Behnken Design (BBD). ANOVA results identified the methanol/WCO molar ratio, reaction temperature, and catalyst loading as the most influential variables, with the methanol/WCO molar ratio showing the highest significance based on its F-value (11.337) and p-value (< 0.0001). The reliability of the quadratic model was validated through statistical parameters, including R^2 (0.9994), R-adj^2 (0.9986), and R-pred^2 (0.9933), confirming an excellent fit with the experimental data. All experiments were conducted with a constant reaction time of 3 h. Under optimal conditions methanol/WCO molar ratio of 11:1, catalyst loading of 2 wt%, and reaction temperature of 60 °C the maximum biodiesel efficiency reached 94.27%. Validation experiments performed in five independent trials yielded an average efficiency of 93.89%, showcasing strong consistency between experimental outcomes and model predictions. The reusability assessment of the αFe_2O_3/CuO nanocatalyst demonstrated its stability, with only a 12% reduction in catalytic efficiency after seven cycles. Future studies should explore the effect of reaction time in conjunction with other parameters for a comprehensive understanding of biodiesel production. Research should also focus on developing more robust catalysts with minimal leaching, and include economic, energy efficiency, and life cycle assessments to evaluate sustainability. These findings position the αFe_2O_3/CuO nanocatalyst as an effective and sustainable solution for biodiesel production, with significant potential for cost-effective industrial-scale applications.

Data availability

All experimental data were published in the current article. The additional data and information will be provided to individuals upon official request to the corresponding author.

Received: 12 December 2024; Accepted: 19 February 2025
Published online: 27 February 2025

References

1. Ghosh, N., Rhithuparna, D., Khatoon, R., Rokhum, S. L. & Halder, G. Sulphonic-acid functionalized novel Limonia acidissima carbonaceous catalyst for biodiesel synthesis from Millettia pinnata oil: optimization, kinetics, thermodynamics and cost analysis. *J. Clean. Prod.* **394**, 136362 (2023).
2. Rhithuparna, D., Ghosh, N., Khatoon, R., Rokhum, S. L. & Halder, G. Evaluating the commercial potential of Cocos nucifera derived Biochar catalyst in biodiesel synthesis from Kanuga oil: optimization, kinetics, thermodynamics, and process cost analysis. *Process Saf. Environ. Prot.* **183**, 859–874 (2024).
3. Alotaibi, M. A. et al. Optimization and cost analysis evaluation studies of the biodiesel production from waste cooking oil using Na–Si/Ce-500 heterogeneous catalyst. *Biomass Bioenerg.* **182**, 107078 (2024).
4. Maleki, B., Esmaeili, H., Yatish, K. V. & Yusuf, M. A critical review on MOFs and COFs-based heterogeneous catalysts in biodiesel generation: synthesis methods, structural features, mechanisms, kinetic, economic/environmental evaluation, and their performance. *Process Saf. Environ. Prot.* **187**, 903–925 (2024).
5. Foroutan, R., Peighambardoust, S. J., Mohammadi, R., Peighambardoust, S. H. & Ramavandi, B. Investigation of kinetics, thermodynamics, and environmental factors of biodiesel generation from sunflower and castor oil using rice husk ash/CuO/K_2CO_3 heterogeneous catalyst. *Environ. Technol. Innov.* **32**, 103307 (2023).
6. Maleki, B. & Talesh, A. Sustainable biodiesel production from wild oak (Quercus Brantii Lindl) oil as a novel and potential feedstock via highly efficient Co@CuO nanocatalyst: RSM optimization and CI engine assessment. *Renew. Energy*. **224**, 120127 (2024).
7. Huang, J., Wang, J., Huang, Z., Liu, T. & Li, H. Photothermal technique-enabled ambient production of microalgae biodiesel: mechanism and life cycle assessment. *Bioresour. Technol.* **369**, 128390 (2023).
8. Arun, S. B. et al. Exploitation of Annona reticulata leaf extract for the synthesis of CeO_2 nanoparticles as catalyst for the generation of biodiesel using seed oil thereof. *Energy* **298**, 131335 (2024).
9. Aziz, A. et al. Novel copper oxide phyto-nanocatalyst utilized for the synthesis of sustainable biodiesel from citrullus colocynthis seed oil. *Processes* **11**, 1857 (2023).
10. Nayab, R. et al. Sustainable biodiesel production via catalytic and non-catalytic transesterification of feedstock materials–A review. *Fuel* **328**, 125254 (2022).
11. Daniyan, I., Bello, E., Ogedengbe, T. & Mpofu, K. Use of central composite design and artificial neural network for predicting the yield of biodiesel. *Procedia CIRP*. **89**, 59–67 (2020).
12. Esmaeili, H. A critical review on the economic aspects and life cycle assessment of biodiesel production using heterogeneous nanocatalysts. *Fuel Process. Technol.* **230**, 107224 (2022).
13. Farid, M. A. A. et al. Kinetic and thermodynamic of heterogeneously K_3PO_4/AC-catalysed transesterification via pseudo-first order mechanism and Eyring-Polanyi equation. *Fuel* **232**, 653–658 (2018).
14. Guo, M., Jiang, W., Ding, J. & Lu, J. Highly active and recyclable CuO/ZnO as photocatalyst for transesterification of waste cooking oil to biodiesel and the kinetics. *Fuel* **315**, 123254 (2022).
15. Maleki, B. & Talesh, A. Pour point and yield simultaneous improvement of alkyl esters produced by ultrasound-assisted in the presence of αFe_2O_3/ZnO: RSM approach. *Fuel* **298**, 120827 (2021).
16. Talebi, M., Larimi, A., Khorasheh, F. & Borhani, T. N. Biodiesel production using heterogeneous catalyst derived from natural calcite stone: study of the effect of Mg–Zr doping and reaction conditions. *Sustainable Chem. Pharm.* **39**, 101559, (2024).
17. Olubunmi, B. E., Alade, A. F., Ebhodaghe, S. O. & Oladapo, O. T. Optimization and kinetic study of biodiesel production from beef tallow using calcium oxide as a heterogeneous and recyclable catalyst. *Energy Convers. Management: X* **14**, 100221, (2022).
18. Maleki, B. & Esmaeili, H. Ultrasound-assisted conversion of waste frying oil into biodiesel using Al-doped ZnO nanocatalyst: Box-Behnken design-based optimization. *Renew. Energy*. **209**, 10–26 (2023).
19. Heidari-Maleni, A., Gundoshmian, T. M., Pakravan-Charvadeh, M. R. & Flora, C. Life cycle assessment of biodiesel production from fish waste oil. *Environ. Challenges*. **14**, 100850 (2024).
20. Sun, X., Xu, L., Yuan, H., Wang, G. & Maleki, B. Boosted conversion of restaurant waste oil into biodiesel using Fe3O4@UiO-66-NH2 magnetic heterogeneous nanocatalyst and its application on the diesel engine: optimization via RSM. *Renew. Energy*. **223**, 120007 (2024).
21. Karimi, K., Saidi, M., Moradi, P. & Taheri Najafabadi, A. Biodiesel production from Nannochloropsis microalgal biomass-derived oil: an experimental and theoretical study using the RSM-CCD approach. *Can. J. Chem. Eng.* **101**, 5600 (2023).
22. Maleki, B., Esmaeili, H., Mansouri, M., Kumar, D. & Singh, B. Enhanced conversion of dairy waste oil to biodiesel via novel and highly reactive UiO-66-NH_2/ZnO/TiO_2 nano-catalyst: optimization, kinetic, thermodynamic and diesel engine studies. *Fuel* **339**, 126901 (2023).
23. Raghavendra, M., Yatish, K. V., Lalithamba, H. S. & Omkaresh, B. R. Effective utilization of green synthesized CuO nanoparticles for the Preparation of keto-1, 2, 3-triazole analogues of protected amino acids/dipeptide acids and recyclable catalyst for the optimization and kinetic study of biodiesel production. *Eur. Phys. J. Plus*. **136**, 1–20 (2021).
24. Zhang, H., Zhou, L. & Huang, X. Y. Upgrading MnO_2@CuO with rGO as a superior heterogeneous nanocatalyst for transesterification of dairy waste oils to biodiesel through electrolysis procedure. *Mater. Today Sustain.* **24**, 100607 (2023).
25. Siavash Moakhar, R. et al. And Riahi-Noori, N. Photoelectrochemical water-splitting using CuO-based electrodes for hydrogen production: a review. *Adv. Mater.* **33**, 2007285 (2021).
26. Krishna, A. M. S. et al. Functionalized Graphene-incorporated cupric oxide charge-transport layer for enhanced photoelectrochemical performance and hydrogen evolution. *Catalysts* **13**, 785 (2023).
27. Karthikeyan, C. & Karuppuchamy, S. Synthesis of novel CuO–Al_2O_3 catalyst for biodiesel production. *Adv. Sci. Eng. Med.* **9**, 1011–1016 (2017).
28. Thakura, N. & Kumar, K. Effect of (Ag, Co) co-doping on the structural and antibacterial efficiency of CuO nanoparticles: A rapid microwave assisted method. *J. Environ. Chem. Eng.* **8**, 104011 (2020).
29. Thakur, N., Anu, Kumar, K. & Sharma, K. K. Application of Co-doped copper oxide nanoparticles against different multidrug resistance bacteria. *Inorg. Nano-Metal Chem.*, 1–12, (2020).
30. Mohamed, R. M., Harraz, F. A. & Shawki, A. CuO nanobelts synthesized by a template-free hydrothermal approach with optical and magnetic characteristics. *Ceram. Int.* **40**, 2127–2133 (2014).
31. Sharma, A., Dutta, R. K., Das, R. A., Goyal, D. A. & Kapoor, A. Cobalt doped CuO nanoparticles as a highly efficient heterogeneous catalyst for reduction of 4-nitrophenol to 4-aminophenol. *App Catal. A: Gen.* **543**, 1–36 (2017).
32. Zeid, E. F. A., Ibrahem, I. A., Mohamed, W. A. A. & Mossad Ali, A. M. Study the influence of silver and Cobalt on the photocatalytic activity of copper oxide nanoparticles for the degradation of Methyl orange and real wastewater dyes. *Mater. Res. Express*. **7**, 1–17 (2020).
33. Babu, M. M. H., Podder, J., Tofa, R. R. & Ali, L. Effect of Co doping in tailoring the crystallite size, surface morphology and optical band gap of CuO thin films prepared via thermal spray pyrolysis. *Surf. Interfaces*. **25**, 101269 (2021).
34. Subhalakshmi, N. & Ganeshwari, K. M. K. Synthesis and characterization of different percentage (Fe^{2+}) doped copper oxide (CuO) NPs prepared by chemical method. *Int. J. Sci. Res. Phy Appl. Sci.* **7**, 348–3423 (2019).

35. Suresh, T., Sivarajasekar, N. & Balasubramani, K. Enhanced ultrasonic assisted biodiesel production from meat industry waste (pig tallow) using green copper oxide nanocatalyst: comparison of response surface and neural network modelling. *Renew. Energy*. **164**, 897–907 (2021).
36. Sulaiman, N. F., Leong, Y. W., Lee, S. L., Goh, Z. W. & Yahya, S. S. M. Process optimization of rice husk Ash supported catalyst in biodiesel synthesis using response surface methodology approach. *Fuel* **358**, 130165 (2024).
37. Zhang, X. RSM-based optimization for ultrasound-assisted transesterification of Jojoba oil to biodiesel via $ZnFe_2O_4$@TiO_2 retrievable nanocatalyst: application on the diesel engine. *Ind. Crops Prod.* **220**, 119144 (2024).
38. Maleki, B., Yatish, K. V., Muthusamy, B. & Esmaeili, H. A cleaner approach towards magnetically assisted-electrolysis of biodiesel production using novel $MnFe_2O_4$@sawdust derived Biochar nanocatalyst and its performance on a CI engine. *Energy. Conv. Manag.* **299**, 117829, (2024).
39. Maleki, B. & Talesh, A. Cold flow properties and CI engine parameters synchronic improvement of biodiesel/diesel/C3 and C4 alcohol blends: mixture design approach. *Process Saf. Environ. Prot.* **160**, 310–326 (2022).
40. Liang, X., Ji, H., Ali, E. & Marzouki, R. Ultrasonic-assisted biodiesel generation from waste chicken fat utilizing reusable Ce-doped Fe_2O_3 nanocatalyst and its utilization as a nano-additive in diesel engine. *Process Saf. Environ. Prot.* **184**, 834–853 (2024).
41. Maleki, B. et al. Novel Co_3O_4 decorated with rGO nanocatalyst to boost microwave-assisted biodiesel production and as nano-additive to enhance the performance-emission characteristics of diesel engine. *Energy* **289**, 129944 (2024).
42. Yatish, K. V., Lalithamba, H. S., Suresh, R. & Latha, H. K. E. Ochrocarpus longifolius assisted green synthesis of $CaTiO_3$ nanoparticle for biodiesel production and its kinetic study. *Renew. Energy*. **147**, 310–321 (2020).
43. Najafi, B., Faizollahzadeh Ardabili, S., Shamshirband, S., Chau, K. W. & Rabczuk, T. Application of ANNs, ANFIS and RSM to estimating and optimizing the parameters that affect the yield and cost of biodiesel production. *Eng. Appl. Comput. Fluid Mech.* **12**, 611–624 (2018).
44. Li, Y. et al. Biomass-derived hydrophobic metal-organic frameworks solid acid for green efficient catalytic esterification of oleic acid at low temperatures. *Fuel Process. Technol.* **239**, 107558 (2023).
45. Maleki, B. et al. A novel biomass derived activated carbon mediated AC@ ZnO/NiO bifunctional nanocatalyst to produce high-quality biodiesel from dairy industry waste oil: CI engine performance and emission. *Chem. Eng. J.* **467**, 143399, (2023).
46. Yatish, K. V. et al. *Terminalia chebula* as a novel green source for the synthesis of copper oxide nanoparticles and as feedstock for biodiesel production and its application on diesel engine. *Energy* **215**, 119165 (2021).
47. Maleki, B. & Ashraf Talesh, S. S. Optimization of ZnO incorporation to αFe_2O_3 nanoparticles as an efficient catalyst for biodiesel production in a sonoreactor: application on the CI engine. *Renew. Energy*. **182**, 43–59 (2022).
48. Man, Y., Habibi, M. & Maleki, B. Biodiesel synthesis from waste coconut scum oil utilizing $SnFe_2O_4$/cigarette butt-derived Biochar as a magnetic nanocatalyst: optimization, kinetic and thermodynamic study. *Chem. Eng. Res. Des.* **210**, 311–327 (2024).
49. Singh, W. R. & Singh, H. N. Maximizing waste cooking oil biodiesel production employing novel brotia costula derived catalyst through statistical and machine learning optimization techniques. *Mater. Today Commun.* **41**, 110838 (2024).
50. Singh, W. R. & Singh, H. N. CCD-RSM optimization of biodiesel production from waste cooking oil using Angulyagra oxytropis and Bellamya crassa snail shell-based heterogeneous catalysts. *Fuel* **378**, 132953 (2024).
51. Singh, W. R. & Singh, H. N. Clean biodiesel production approach using waste Swan eggshell derived heterogeneous catalyst: an optimization study employing Box-Behnken-response surface methodology. *Ind. Crops Prod.* **220**, 119181 (2024).
52. Alaei, S., Haghighi, M., Toghiani, J. & Vahid, B. R. Magnetic and reusable MgO/$MgFe_2O_4$ nanocatalyst for biodiesel production from sunflower oil: influence of fuel ratio in combustion synthesis on catalytic properties and performance. *Ind. Crops Prod.* **117**, 322–332 (2018).
53. Ruatpuia, J. V. et al. Microwave-assisted biodiesel production using ZIF-8 MOF-derived nanocatalyst: A process optimization, kinetics, thermodynamics and life cycle cost analysis. *Energy. Conv. Manag.* **292**, 117418 (2023).
54. Maleki, B., Esmaeili, H., Yatish, K. V. & Amruth, E. Valorization of dairy waste scum oil and rice husk ash-supported CuO nanocatalyst towards cleaner production of biodiesel: A waste-to-energy approach. *Process Saf. Environ. Prot.* **192** (2024), 1393–1407 (2024).
55. Tamjidi, S., Moghadas, B. K. & Esmaeili, H. Ultrasound-assisted biodiesel generation from waste edible oil using $CoFe_2O_4$@GO as a superior and reclaimable nanocatalyst: optimization of two-step transesterification by RSM. *Fuel* **327**,125170, (2022).
56. Tamjidi, S., Esmaeili, H. & Moghadas, B. K. Performance of functionalized magnetic nanocatalysts and feedstocks on biodiesel production: a review study. *J. Clean. Prod.* **305**, 127200 (2021).
57. Yatish, K. V., Lalithamba, H. S., Suresh, R., Arun, S. B. & Kumar, V. Optimization of scum oil biodiesel production by using response surface methodology. *Process. Saf. Environ. Prot.* **102**, 667–672 (2016).
58. Sun, C. et al. Comparison of biodiesel production using a novel porous Zn/Al/Co complex oxide prepared from different methods: physicochemical properties, reaction kinetic and thermodynamic studies. *Renew. Energy*. **181**, 1419–1430 (2022).
59. Zhang, Y., Duan, L. & Esmaeili, H. A review on biodiesel production using various heterogeneous nanocatalysts: operation mechanisms and performances. *Biomass Bioenerg.* **158**, 106356 (2022).

Author contributions

All authors contributed to the study conception and design. Material preparation, data collection and analysis were performed by A.R., M.M., and B.M. The first draft of the manuscript was written by M.M. and all authors commented on previous versions of the manuscript. All authors read and approved the final manuscript. All authors are fully aware of this manuscript and have permission to submit the manuscript for possible publication.

Declarations

Competing interests

The authors declare no competing interests.

Additional information

Correspondence and requests for materials should be addressed to M.M.

Reprints and permissions information is available at www.nature.com/reprints.

Publisher's note Springer Nature remains neutral with regard to jurisdictional claims in published maps and institutional affiliations.